J. Fluid Mech. (1986), *vol.* 168, *pp.* 169–194
Printed in Great Britain

The dynamics of the spreading of liquids on a solid surface. Part 1. Viscous flow

By R. G. COX
Department of Civil Engineering and Applied Mechanics, McGill University, Montreal, PQ, Canada

(Received 25 August 1983 and in revised form 2 December 1985)

An investigation is made into the dynamics involved in the movement of the contact line when one liquid displaces an immiscible second liquid where both are in contact with a smooth solid surface. In order to remove the stress singularity at the contact line, it has been postulated that slip between the liquid and the solid or some other mechanism must occur very close to the contact line. The general procedure for solution is described for a general model for such slip and also for a general geometry of the system. Using matched asymptotic expansions, it is shown that for small capillary number and for small values of the length over which slip occurs, there are either 2 or 3 regions of expansion necessary depending on the limiting process being considered. For the very important situation where 3 regions occur, solutions are obtained from which it is observed that in general there is a maximum value of the capillary number for which the solutions exist. The results obtained are compared with existing theories and experiments.

1. Introduction

Consider two immiscible liquids (liquid A and liquid B) or a liquid and a gas in contact with a solid surface (or solid surfaces) and suppose that liquid A displaces liquid B so that the contact line [where the liquid–liquid interface intersects the solid surface] is constrained to move across the solid surface with a velocity U. Then the observed contact angle (that the liquid–liquid interface makes with the solid surface), which we will measure through liquid A, is known to increase as U increases [Dussan V. 1979]. We will consider here the dynamics of this contact-line movement and will, for simplicity, assume that the solid surface (or surfaces) involved are perfectly smooth and chemically homogeneous. However it must be admitted that while roughness and chemical heterogeneity of the solid are suspected to be at least partly responsible for the jump in value of the contact angle (i.e.contact-angle hysteresis) occurring in the static limit of $U = 0$ (Johnson & Dettre 1964; Huh & Mason 1977*a*; Cox 1983), it is not known what effect these might have for a non-zero spreading velocity U. We will consider a completely general geometry for the system under discussion since we are primarily interested here in what happens very close to the contact line and we expect that this, to some extent, will not depend on the overall geometry. Thus we might have for example (*a*) the spreading of a drop on a horizontal surface (Greenspan 1978; Hocking & Rivers 1982), (*b*) the movement of a drop down an inclined surface, (*c*) the movement of a meniscus along a tube of circular or non-circular cross-section, (*d*) the movement of some object (e.g. plate, cylinder, sphere) through a liquid–liquid interface or (*e*) the squeezing of a drop between two parallel plates.

When the flow field is calculated in the neighbourhood of a moving contact line it is found that there is a non-integrable singularity in the stress at the contact line resulting in a divergent integral for the drag force on the solid boundary. In order to avoid this problem slip has been postulated to occur between the liquids and the solid surface close to the contact line (Hocking 1977; Huh & Mason 1977*b*). The following models for this slip have been used:

(i) Zero tangential stress at the solid surface at distances from the contact line less than s and no slip for distances greater than s (Huh & Mason 1977*b*). This slip length may possibly be different in the two liquids being s in liquid A and αs in liquid B (where α is assumed to be of order unity).
(ii) Difference in tangential velocity between liquid and solid equal to s times the shear velocity gradient at the solid surface (Hocking 1977; Huh & Mason 1977*b*; Lowndes 1980).

A more general model might be

(iii) Difference in tangential velocity between liquid and solid equal to s^p-times the shear velocity gradient at the solid surface to the power of p (where $p > 0$).

In all these models s is a measure of the distance from the contact line over which slip occurs. It should be mentioned that slip between liquid and solid is a convenient assumption to get rid of the non-integrable stress singularity, but that there are also other possibilities such as non-continuum effects, non-Newtonian fluid effects and the elasticity of the solid, which might also have the effect of removing the singularity.

For a specific slip model and specific overall geometry, this problem has been examined for small capillary number and small ratio of slip length s to macroscopic lengthscale. This has been done using singular perturbation methods using two regions of expansion (Hocking 1977; Huh & Mason 1977*b*) and using three regions of expansion (Hocking & Rivers 1982). After a discussion of the outer region (§3) in which the overall geometry is important and the inner region (§4) applicable close to the contact line (at distances of order s), a discussion is given (§5) of the conditions necessary for a two-region expansion or a three-region expansion to be valid. It is shown that whereas for the two-region expansion, the observed contact angle must be approximately the static value, this is not the case for the three-region expansion, and so we examine here in detail the more interesting situation of the three-region expansion. Thus, in addition to the outer and inner regions mentioned above, we have an intermediate region lying between them as described by Hocking & Rivers (1982). Since in this intermediate region we are considering lengthscales small compared with the macroscopic dimension of the overall system but large compared with the slip length s, we can at lowest order, solve without consideration of the overall geometry or the slip model used. This is done in §6. Then upon matching the intermediate region solution onto the inner and outer region expansions the general solution is obtained in §7. Since it is found that the major contribution to the effect on the contact angle comes from the intermediate region, we find that at lowest order in the capillary number the solution obtained is independent of the solution in the inner and outer regions. Furthermore, even at the next higher order in the capillary number, the solution is dependent only upon one constant obtained from the inner region solution (which is thus dependent on the slip model used) and one constant obtained from the outer region solution (which is thus dependent on the overall geometry of the system). Finally in §8, a general discussion of the results is given including conditions of validity and a comparison with existing theories and experiments. Details are also given concerning the flow field in the intermediate region.

2. General problem

Let R be some characteristic macroscopic length and U some characteristic velocity for the flow occurring when liquid A (of viscosity μ_A and density ρ_A) displaces liquid B (of viscosity μ_B and density ρ_B). During this motion, slip between each liquid and the solid surface (or some other mechanism to get rid of the non-integrable stress singularity) must occur at distances of order s from the contact line. Since we expect s to be very small, possibly of molecular size, it is reasonable to assume that

$$\epsilon \equiv \frac{s}{R} \ll 1. \tag{2.1}$$

In addition it will be assumed that the tension σ of the interface between the two liquids is sufficiently large that interfacial tension effects dominate over viscous effects, or more precisely that the capillary numbers for the two liquids are small, i.e.

$$Ca \equiv \frac{\mu_A U}{\sigma} \ll 1, \tag{2.2a}$$

$$\lambda Ca \equiv \frac{\mu_B U}{\sigma} \ll 1. \tag{2.2b}$$

where $\lambda \equiv \mu_B/\mu_A$ is the viscosity ratio of the liquids. In making a double expansion in terms of the two parameters ϵ and Ca [or ϵ and λCa if $\lambda \gg 1$], it will be shown later that either 2 or 3 regions of expansion are necessary depending on the manner in which one approaches the limit $\epsilon \to 0$, $Ca \to 0$.

The Reynolds numbers $(\rho_A RU/\mu_A)$ and $(\rho_B RU/\mu_B)$ for the flow in the two liquids are assumed to be so small that inertia effects may be neglected. In addition it will be assumed that at all points on the contact line the solid surface is planar on a lengthscale much smaller than R. However the solid surface (or surfaces) present are permitted to be non-planar on a lengthscale of order R since this can be taken into account in the outer region.

3. Outer region

An outer region of expansion is defined using variables made dimensionless by the quantities R, U and μ_A, so that it is valid everywhere except close to the contact line. Thus if $\boldsymbol{u}_A$ and p_A are the dimensionless velocity and pressure in liquid A and $\boldsymbol{u}_B$ and p_B the dimensionless velocity and pressure in liquid B in this outer expansion, and if $\boldsymbol{r}$ is the dimensionless position vector, then in the absence of gravity effects [i.e. if the Bond number $B \equiv |\rho_A - \rho_B| gR^2/\sigma$ is very small],

$$\nabla^2 \boldsymbol{u}_A - \nabla p_A = 0 \quad \nabla \cdot \boldsymbol{u}_A = 0, \tag{3.1}$$

in liquid A and

$$\lambda \nabla^2 \boldsymbol{u}_B - \nabla p_B = 0 \quad \nabla \cdot \boldsymbol{u}_B = 0, \tag{3.2}$$

in liquid B. Should the Bond number B be of order unity so that gravity may no longer be neglected, then (3.1) and (3.2) are still valid so long as p_A and p_B are interpreted as the excess pressure over hydrostatic. For the slip model (i) referred to in §1, both $\boldsymbol{u}_A$ and $\boldsymbol{u}_B$ in this outer expansion must satisfy the no-slip boundary condition on all solid walls, since slip only occurs at a distance of $O(\epsilon)$ from the contact line and the flow at such positions will be found by defining an inner region of expansion valid there. However for the slip models (ii) and (iii) referred to in §1, $\boldsymbol{u}_A$

and $\boldsymbol{u}_B$ would satisfy the no-slip boundary condition only at order ϵ^0 as $\epsilon \to 0$. On the interface between the two liquids, the following boundary conditions will apply: (i) The kinematic boundary condition relating the normal velocity at the interface in both liquids to the interface motion; (ii) the continuity of tangential velocity; (iii) the continuity of tangential stress, and (iv) the balance of the normal fluid stress on the interface by the interfacial tension times the mean curvature of the interface.

For a unique solution additional boundary conditions are usually necessary. Such boundary conditions may, for example, involve the statement of a given volume of one of the liquids (as for a drop spreading on a solid surface), of a given pressure drop across the interface (as for a meniscus moving along a tube under a given pressure drop) or of a given flow rate (as for a meniscus moving along a tube at a given velocity). Since the normal-stress difference can be non-zero (and of order σ/R) even in the static situation, its dimensionless value is of the form

$$(\text{normal stress difference due to the flow}) + Ca^{-1}\Delta P, \tag{3.3}$$

where ΔP is of the order unity and is the static pressure drop across the interface (in going from liquid A to liquid B) made dimensionless by σ and R. Thus ΔP is a constant if the Bond number is small so that gravity effects are absent, but is of the form $(a - Bz)$ if the Bond number B is of order unity (a is a constant and z the vertical coordinate). Thus the normal-stress boundary condition in outer variables is

$$Ca\,[\text{normal-stress difference across interface}] + \Delta P = [\text{mean curvature of inter face}], \tag{3.4}$$

and this is the only place where the capillary number Ca appears in the equations and boundary conditions. Thus the liquid velocity $\boldsymbol{u}_A$ (and $\boldsymbol{u}_B$) can be expanded in the form

$$\boldsymbol{u}_A = \boldsymbol{u}_{A0} + Ca\,\boldsymbol{u}_{A1} + \dots, \tag{3.5}$$

whilst the liquid–liquid interface $f(\boldsymbol{r}) = 0$ in these outer variables can be expanded as

$$f \equiv f_0 + Ca f_1 + \dots = 0, \tag{3.6}$$

where $\boldsymbol{u}_{A0}$, $\boldsymbol{u}_{A1}$, f_0, f_1 etc. will in general be functions of ϵ since (i) ϵ may become involved through the required matching at the contact line (discussed in §5) and (ii) the slip boundary condition at the walls may involve ϵ. Thus these quantities may be expanded in terms of ϵ. By substituting the expansions (3.5) and (3.6) into (3.1) and (3.2) and the boundary conditions, it is seen that $f_0 = 0$ is just the static position of the interface determined by the normal-stress boundary condition at lowest order, namely,

$$\Delta P = [\text{mean curvature of interface}]. \tag{3.7}$$

Thus f_0 is independent of ϵ whilst it is seen that $\boldsymbol{u}_{A0}$ expanded in terms of ϵ must be of the form

$$\boldsymbol{u}_{A0}(\boldsymbol{r}, \epsilon) = \boldsymbol{u}_{A00}(\boldsymbol{r}) + o(1) \quad \text{as } \epsilon \to 0, \tag{3.8}$$

where $\boldsymbol{u}_{A00}$ is independent of ϵ. The precise order of the $o(1)$ terms in (3.8) depends on the slip model used. At present $f_0 = 0$ is just any static interface configuration about which we are expanding. The determination of such a static configuration would require specification of the contact line position and also a subsidiary boundary condition of the type mentioned previously (e.g. given drop volume for a drop spreading on a solid surface). We assume that the contact-line position is known although in most problems it would not be known *a priori*.

The zeroth-order velocity fields $\boldsymbol{u}_{A00}, \boldsymbol{u}_{B00}$ can then be found by solving (3.1) and (3.2) and all the boundary conditions (other than the normal-stress condition)

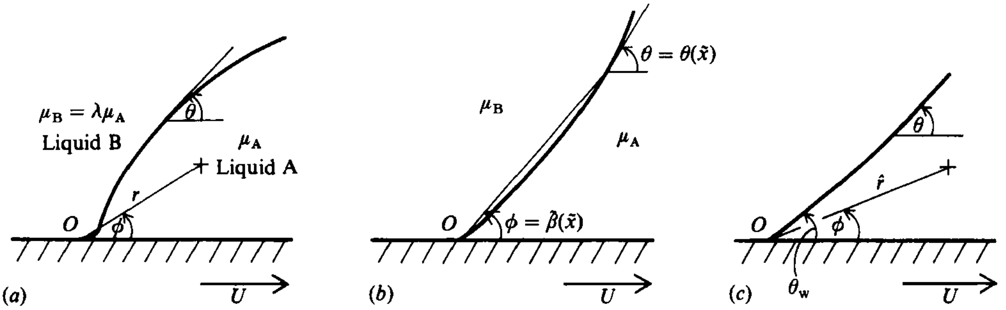

FIGURE 1. (*a*) Outer region: coordinates are (r, ϕ) and interface slope is θ. (*b*) Intermediate region: coordinates are $(\tilde{x}, \phi)$ where $\tilde{x} = Ca \ln r$ and interface $\phi = \tilde{\beta}(\tilde{x})$ has slope $\theta = \theta(\tilde{x})$. (*c*) Inner region: coordinates are $(\hat{r}, \phi)$ where $\hat{r} = \epsilon^{-1} r$.

with the interface given by the known static position $f_0 = 0$. Then from these values of $\boldsymbol{u}_{A00}, \boldsymbol{u}_{B00}$ the normal-stress difference across the interface due to this flow can be calculated and hence, by the normal-stress condition at order Ca^{+1}, the value of the interface shape correction f_1 found. In order that for a given f_0, the value of f_1 be unique, we assume that the surfaces $f_0 = 0$ and $f_0 + Ca f_1 = 0$ have the same contact line position and the same subsidiary boundary condition (e.g. given drop volume or given pressure difference across the interface).

For systems with simple geometry, it may sometimes be possible to obtain explicit values for f_0, $\boldsymbol{u}_{A00}$, $\boldsymbol{u}_{B00}$ and f_1 as was done by Hocking & Rivers (1982) for the case of a drop spreading on a plane surface. However for more complicated situations it is very difficult to calculate even the static interface shape given by f_0. Thus here, since we are more interested in behaviour close to the contact line, we will calculate the asymptotic form of the interface shape (3.5) as the contact line is approached since it is this which is needed for the matching procedure close to the contact line. Thus if O is the point which we wish to consider on the line of intersection of $f_0 = 0$ with the solid surface (i.e. on the zeroth-order contact line position), we set up a cylindrical polar coordinate system (r, ϕ, z) in outer variables with origin at O and moving with the contact line (see figure 1*a*) and z-axis lying tangent to the contact line with $\phi = 0$ in the solid surface in the direction opposite to that of contact line motion (for $U > 0$). For the purpose of investigating the flow in the neighbourhood of O, we can choose the characteristic speed U as the speed of the contact line at O, so that in our local (r, ϕ, z) variables, the wall moves in the direction $\phi = 0$ with unit velocity.

Consider first the static position $f_0 = 0$ of the interface determined by (3.6). In the (r, ϕ)-plane, if the angle at which this static interface meets the solid surface is θ_m for $r \to 0$, then

$$\theta = \theta_m + O(r), \tag{3.9}$$

where θ is the angle the tangent plane to the interface makes with the solid surface at a general position (see figure 1*a*). When r is sufficiently small, this interface may be taken as the plane $\phi = \theta_m$. The asymptotic form of the velocity field as $r \to 0$ can be obtained by defining stream functions ψ_A and ψ_B for liquids A and B such that $(u_{A00})_r$ and $(u_{A00})_\phi$, the radial and transverse components of $\boldsymbol{u}_{A00}$ are

$$(u_{A00})_r = \frac{1}{r}\frac{\partial \psi_A}{\partial \phi} \quad (u_{A00})_\phi = -\frac{\partial \psi_A}{\partial r}, \tag{3.10}$$

with similar expressions for the components of $\boldsymbol{u}_{\mathrm{B}00}$. If these values are substituted into (3.1) and (3.2), we obtain, upon the elimination of the pressure

$$\nabla^4\psi_{\mathrm{A}} = 0 \quad \text{and} \quad \nabla^4\psi_{\mathrm{B}} = 0. \tag{3.11}$$

The no-slip boundary condition on the solid wall gives

$$\psi_{\mathrm{A}} = 0 \quad \frac{\partial\psi_{\mathrm{A}}}{\partial\phi} = +r \text{ on } \phi = 0, \tag{3.12}$$

$$\psi_{\mathrm{B}} = 0 \quad \frac{\partial\psi_{\mathrm{B}}}{\partial\phi} = -r \text{ on } \phi = \pi, \tag{3.13}$$

while the boundary conditions for $\boldsymbol{u}_{\mathrm{A}00}$ and $\boldsymbol{u}_{\mathrm{B}00}$ at the interface $\phi = \theta_{\mathrm{m}}$ with zero normal velocity (to be justified later) reduce to:

$$\frac{\partial\psi_{\mathrm{A}}}{\partial r} = \frac{\partial\psi_{\mathrm{B}}}{\partial r} = 0, \tag{3.14}$$

$$\frac{\partial\psi_{\mathrm{A}}}{\partial\phi} = \frac{\partial\psi_{\mathrm{B}}}{\partial\phi}, \tag{3.15}$$

$$\left(\frac{1}{r^2}\frac{\partial^2\psi_{\mathrm{A}}}{\partial\phi^2} - \frac{\partial^2\psi_{\mathrm{A}}}{\partial r^2} + \frac{1}{r}\frac{\partial\psi_{\mathrm{A}}}{\partial r}\right) = \lambda\left(\frac{1}{r^2}\frac{\partial^2\psi_{\mathrm{A}}}{\partial\phi^2} - \frac{\partial^2\psi_{\mathrm{B}}}{\partial r^2} + \frac{1}{r}\frac{\partial\psi_{\mathrm{B}}}{\partial r}\right). \tag{3.16}$$

The solution of (3.11) of the form required in order to satisfy the boundary conditions (3.12) and (3.13) is

$$\begin{aligned}\psi_{\mathrm{A}} &= r\{(C_{\mathrm{A}}\phi + D_{\mathrm{A}})\cos\phi + (E_{\mathrm{A}}\phi + F_{\mathrm{A}})\sin\phi\},\\ \psi_{\mathrm{B}} &= r\{(C_{\mathrm{B}}\phi + D_{\mathrm{B}})\cos\phi + (E_{\mathrm{B}}\phi + F_{\mathrm{B}})\sin\phi\},\end{aligned} \tag{3.17}$$

where C_{A}, D_{A}, E_{A}, etc. are constants which can be determined using the boundary conditions (3.12) to (3.16) as

$$\begin{aligned}
C_{\mathrm{A}} &= \sin\theta_{\mathrm{m}}\,[-\lambda\{\pi\sin\theta_{\mathrm{m}} + \sin^2\theta_{\mathrm{m}}\cos\theta_{\mathrm{m}} + \theta_{\mathrm{m}}(\pi-\theta_{\mathrm{m}})\cos\theta_{\mathrm{m}}\}\\
&\qquad + \cos\theta_{\mathrm{m}}\{+\sin^2\theta_{\mathrm{m}} - (\pi-\theta_{\mathrm{m}})^2\}]/\Delta,\\
D_{\mathrm{A}} &= 0,\\
E_{\mathrm{A}} &= \sin^2\theta_{\mathrm{m}}\,[-\lambda\{\sin^2\theta_{\mathrm{m}} + \theta_{\mathrm{m}}(\pi-\theta_{\mathrm{m}})\} + \{+\sin^2\theta_{\mathrm{m}} - (\pi-\theta_{\mathrm{m}})^2\}]/\Delta,\\
F_{\mathrm{A}} &= \theta_{\mathrm{m}}\,[+\lambda\{\sin^2\theta_{\mathrm{m}} + \theta_{\mathrm{m}}(\pi-\theta_{\mathrm{m}}) + \pi\sin\theta_{\mathrm{m}}\cos\theta_{\mathrm{m}}\} + \{-\sin^2\theta_{\mathrm{m}} + (\pi-\theta_{\mathrm{m}})^2\}]/\Delta,\\
-D_{\mathrm{B}}/\pi = C_{\mathrm{B}} &= \sin\theta_{\mathrm{m}}\,[+\lambda\cos\theta_{\mathrm{m}}(\theta_{\mathrm{m}}^2 - \sin^2\theta_{\mathrm{m}})\\
&\qquad + \{-\pi\sin\theta_{\mathrm{m}} + \sin^2\theta_{\mathrm{m}}\cos\theta_{\mathrm{m}} + \theta_{\mathrm{m}}(\pi-\theta_{\mathrm{m}})\cos\theta_{\mathrm{m}}\}]/\Delta,\\
E_{\mathrm{B}} &= \sin^2\theta_{\mathrm{m}}\,[+\lambda(\theta_{\mathrm{m}}^2 - \sin^2\theta_{\mathrm{m}}) + \{+\sin^2\theta_{\mathrm{m}} + \theta_{\mathrm{m}}(\pi-\theta_{\mathrm{m}})\}]/\Delta,\\
F_{\mathrm{B}} &= [\lambda(-\theta_{\mathrm{m}}^2 + \sin^2\theta_{\mathrm{m}})(\theta_{\mathrm{m}} - \pi\cos^2\theta_{\mathrm{m}}) + \{-\pi(\pi-\theta_{\mathrm{m}})\sin\theta_{\mathrm{m}}\cos\theta_{\mathrm{m}}\\
&\qquad - \theta_{\mathrm{m}}\sin^2\theta_{\mathrm{m}} + \pi\sin^2\theta_{\mathrm{m}}\cos^2\theta_{\mathrm{m}} + \pi(\pi-\theta_{\mathrm{m}})\theta_{\mathrm{m}}\cos^2\theta_{\mathrm{m}} - (\pi-\theta_{\mathrm{m}})\theta_{\mathrm{m}}^2\}]/\Delta,
\end{aligned} \tag{3.18}$$

where

$$\begin{aligned}\Delta = \lambda(\theta_{\mathrm{m}}^2 - \sin^2\theta_{\mathrm{m}})\{(\pi-\theta_{\mathrm{m}}) + \sin\theta_{\mathrm{m}}\cos\theta_{\mathrm{m}}\}\\ + \{(\pi-\theta_{\mathrm{m}})^2 - \sin^2\theta_{\mathrm{m}}\}(\theta_{\mathrm{m}} - \sin\theta_{\mathrm{m}}\cos\theta_{\mathrm{m}}).\end{aligned} \tag{3.19}$$

The normal stress on the interface $\phi = \theta_{\mathrm{m}}$ directed in the positive ϕ-direction due to this flow is found to be

$$-2r^{-1}[(\lambda C_{\mathrm{B}} - C_{\mathrm{A}})\cos\theta_{\mathrm{m}} + (\lambda E_{\mathrm{B}} - E_{\mathrm{A}})\sin\theta_{\mathrm{m}}] = -r^{-1}f(\theta_{\mathrm{m}}, \lambda), \tag{3.20}$$

where the function $f(\theta, \lambda)$ is obtained as

$$f(\theta,\lambda) \equiv \frac{2\sin\theta[\lambda^2(\theta^2-\sin^2\theta)+2\lambda\{\theta(\pi-\theta)+\sin^2\theta\}+\{(\pi-\theta)^2-\sin^2\theta\}]}{\lambda(\theta^2-\sin^2\theta)\{(\pi-\theta)+\sin\theta\cos\theta\}+\{(\pi-\theta)^2-\sin^2\theta\}(\theta-\sin\theta\cos\theta)}. \quad (3.21)$$

In addition to the term (3.20), the normal stress on the liquid–liquid interface may also be expected to contain terms which are non-singular as $r \to 0$ arising from the flow in the corner induced by the overall flow in the outer region away from the contact line (and also to the fact that the interface is only planar in the limit $r \to 0$). It should be noted that in situations where the interface configuration changes in time with a characteristic timescale T, that since $\mathrm{d}\theta_m/\mathrm{d}t$ would be of order T^{-1}, the dimensional normal stress on the interface near the contact line due to this unsteadiness would be of order μT^{-1} compared with the order $\mu U/(Rr)$ due to contact line movement considered here (r is dimensionless outer variable). Thus the effect of unsteadiness is negligible so long as

$$T \gg \frac{Rr}{U}, \quad (3.22)$$

and this will be the case for all r (including $r \to 0$) so long as

$$T \text{ is of order } \frac{R}{U} \text{ or larger} \quad (3.23)$$

The curvature of the liquid–liquid interface can be taken into account by expanding, for small r, the boundary conditions on that interface. One would then obtain additional terms of order r^{+1} in (3.14), r^{+2} in (3.15) and r^0 in the (3.16) giving rise to a term of order r^0 (or possibly of order $\ln r$) in the expression (3.20) for the normal stress.

Since the static interface shape is given by (3.9), the interface configuration for $r \to 0$, correct to order Ca^{+1} can be written as

$$\theta = \{\theta_m + O(r)\} + Ca\,\theta_1 + \dots, \quad (3.24)$$

where from the coefficient of Ca^{+1} in the normal-stress boundary condition (3.4) we

$$\frac{\partial\theta_1}{\partial r} = r^{-1}f(\theta_m, \lambda) + o(r^{-1}). \quad (3.25)$$

From earlier remarks it is seen that the $o(r^{-1})$ term in this equation is really of order r^0 (or possibly of order $\ln r$). Thus integrating (3.25) and substituting the resulting value of θ into (3.24) we obtain the asymptotic form of the liquid–liquid interface for $r \to 0$ as

$$\theta = \{\theta_m + \dots\} + Ca\{f(\theta_m, \lambda)\ln r + Q_0^* + \dots\} + \dots, \quad (3.26)$$

where Q_0^* depends on λ, θ_m, $\mathrm{d}\theta_m/\mathrm{d}t$, and on the entire geometry involved in the outer region. In the above calculation we have expanded the liquid–liquid interface shape about a static position for which, at the point on the contact line being considered, this static interface configuration intersects the solid surface at an angle θ_m. However in the procedure of matching onto a solution valid close to the contact line it will be found (see §5) that the value of this as yet unknown constant θ_m is a function of Ca and may thus be expanded as

$$\theta_m = \theta_{m0} + Ca\,\theta_{m1} + \dots. \quad (3.27)$$

Then (3.26) takes the form

$$\theta = \{\theta_{m0} + \dots\} + Ca\{f(\theta_{m0})\ln r + Q_0^* + \theta_{m1} + \dots\} + \dots. \quad (3.28)$$

4. Inner region

Close to the contact line, an inner region of expansion is defined using variables made dimensionless by the quantities s, U and μ_A. We thus use polar coordinates $(\hat{r}, \phi)$ [with origin at O moving with the contact line], as independent variables so that†

$$\hat{r} \sim \epsilon^{-1} r \quad \text{as } \hat{r} \to \infty. \tag{4.1}$$

The velocity fields $\boldsymbol{u}_A$ and $\boldsymbol{u}_B$ are used (these being identical to those used in the outer region) and are expanded for small Ca as

$$\left.\begin{aligned} \boldsymbol{u}_A &= \hat{\boldsymbol{u}}_{A0}(\hat{r}, \phi; \epsilon) + Ca\, \hat{\boldsymbol{u}}_{A1}(\hat{r}, \phi; \epsilon) + \dots, \\ \boldsymbol{u}_B &= \hat{\boldsymbol{u}}_{B0}(\hat{r}, \phi; \epsilon) + Ca\, \hat{\boldsymbol{u}}_{B1}(\hat{r}, \phi; \epsilon) + \dots, \end{aligned}\right\} \tag{4.2}$$

where $\boldsymbol{u}_{A0}$, $\hat{\boldsymbol{u}}_{B0}$ etc. will in general depend on ϵ. The liquid–liquid interface shape [figure 1c] can be written as $\theta = \theta(\hat{r})$ where θ is defined as in the outer region as being the angle between the interface and the solid surface at a general position. Thus we expand for small Ca as

$$\theta = \hat{\theta}_0(\hat{r}; \epsilon) + Ca\, \hat{\theta}_1(\hat{r}; \epsilon) + \dots. \tag{4.3}$$

The normal-stress boundary condition at the liquid–liquid interface which, in dimensional form is $\mu U/s$ (normal-stress difference in inner variables) + $(\sigma/R)\Delta P = \sigma/s$ (mean curvature of interface in inner variables), can be written in terms of inner variables as

$$Ca[\text{normal stress difference}] + \epsilon\Delta P = [\text{mean curvature of interface}]. \tag{4.4}$$

Thus at order Ca^0, the interface $\theta = \hat{\theta}_0(\hat{r})$ has a curvature of order ϵ^{+1} in inner variables so that the expansion for $\hat{\theta}_0$ in terms of ϵ is

$$\hat{\theta}_0 \sim \theta_w + O(\epsilon\hat{r}) \quad \text{as } \epsilon \to 0. \tag{4.5}$$

Hence the interface is approximately planar and makes an angle θ_w with the solid surface. This angle θ_w will be called the *microscopic* contact angle, its value being determined by the forces acting very near the contact line between the molecules of the two liquid phases and of the solid phase. It is, as already mentioned in the introduction, being assumed that no contact angle hysteresis occurs so that θ_w is the unique static contact angle for the system. It is uncertain whether such an angle θ_w would depend on the spreading velocity U. However, it is to be expected that for the situation not considered here where surfactants are present, θ_w will depend on U since the flow will affect the subfractant concentration at the contact line and hence the value of θ_w. Also some authors [Cherry & Holmes 1969; Blake & Haynes 1969] have suggested that the flow might affect θ_w even for pure systems.

If the lowest-order flow fields $\hat{\boldsymbol{u}}_{A0}$ and $\hat{\boldsymbol{u}}_{B0}$ are expanded for small ϵ, it is seen that they must be of the form

$$\left.\begin{aligned} \hat{\boldsymbol{u}}_{A0} &= \hat{\boldsymbol{u}}_{A00}(\hat{r}, \phi) + o(1), \\ \hat{\boldsymbol{u}}_{B0} &= \hat{\boldsymbol{u}}_{B00}(\hat{r}, \phi) + o(1) \quad \text{as } \epsilon \to 0. \end{aligned}\right\} \tag{4.6}$$

where $\hat{\boldsymbol{u}}_{A00}$ and $\hat{\boldsymbol{u}}_{B00}$ have stream functions $\hat{\psi}_A$ and $\hat{\psi}_B$ respectively [since flow is planar at order ϵ^0]. Then

$$\nabla^4 \hat{\psi}_A = 0, \quad \nabla^4 \hat{\psi}_B = 0, \tag{4.7}$$

† $\hat{r} \neq \epsilon^{-1} r$ since origin used here is at the actual contact line whereas in §3 it was taken at the intersection of $f_0 = 0$ with the solid surface.

while on the liquid–liquid interface $\phi = \theta_w$, they satisfy boundary conditions similar to (3.14), (3.15) and (3.16) [with $\hat{\psi}_A$ and $\hat{\psi}_B$ replacing ψ_A and ψ_B respectively]. Should the interface configuration be time-dependent, then the condition (3.22) for the neglect of this unsteadiness takes the form

$$T \gg \frac{R\epsilon}{U}$$

which is automatically satisfied if (3.23) is satisfied. The boundary conditions on the solid wall [$\phi = 0$ and $\phi = \pi$] are zero normal velocity, i.e.

$$\hat{\psi}_A = 0 \quad \text{on } \phi = 0, \tag{4.8}$$

$$\hat{\psi}_B = 0 \quad \text{on } \phi = \pi, \tag{4.9}$$

and the given slip law, which for the model (i) mentioned in §1 (with the same slip length s in the two liquids) would give

$$\frac{\partial^2 \hat{\psi}_A}{\partial \phi^2} = 0 \quad \text{if } \hat{r} < 1 \quad \frac{\partial \hat{\psi}_A}{\partial \phi} = +\hat{r} \quad \text{if } \hat{r} > 1 \text{ on } \phi = 0, \tag{4.10}$$

$$\frac{\partial^2 \hat{\psi}_B}{\partial \phi^2} = 0 \quad \text{if } \hat{r} < 1 \quad \frac{\partial \hat{\psi}_B}{\partial \phi} = -\hat{r} \quad \text{if } \hat{r} > 1 \text{ on } \phi = \pi. \tag{4.11}$$

Since the flow fields $\hat{\boldsymbol{u}}_{A0}$ and $\hat{\boldsymbol{u}}_{B0}$ and hence also the interface shape correction $\hat{\theta}_1(\hat{r})$ at order Ca^{+1}, depend on the particular model chosen for the slip law, we will not calculate these quantities. Instead we will derive only the asymptotic form of the solution for $\hat{r} \to \infty$. since it is this which is required for the matching procedure.

For large $\hat{r}$, the slip boundary condition applicable on the solid surface must approach the no-slip boundary condition (whatever the chosen slip model may be). Then, by solving in a manner similar to that discussed in §3 using such a no-slip boundary condition, we obtain the normal stress on the interface $\phi = \theta_w$ directed in the positive ϕ-direction due to this flow as $-\hat{r}^{-1}f(\theta_w, \lambda)$ so that the correction $\hat{\theta}_1(\hat{r})$ to the interface shape satisfies

$$\frac{\partial \theta_1}{\partial \hat{r}} \sim \hat{r}^{-1} f(\theta_w, \lambda) \quad \text{as } \hat{r} \to \infty, \tag{4.12}$$

giving
$$\hat{\theta}_1 \sim f(\theta_w, \lambda) \ln \hat{r} + Q_1^* + \dots \quad \text{as } \hat{r} \to \infty, \tag{4.13}$$

where the integration constant Q_1^* is determined by a knowledge of the entire flow field in the inner region. Terms which tend to 0 slower than $\hat{r}^{-1}$ as $\hat{r} \to \infty$ cannot appear in (4.12) since they would give rise to terms which would tend to ∞ faster than $\ln \hat{r}$ in (4.13). Such terms cannot appear since they would match onto terms in the coefficient of Ca in (3.28) which would tend to ∞ as $\epsilon \to 0$. Even for the three-region expansion situation discussed in §5 it is seen that such terms cannot appear since they would match onto terms in the intermediate region which would tend to ∞ as $\epsilon \to 0$. Indeed the inner solutions obtained by Huh & Mason (1977*b*), Hocking (1977) and Hocking & Rivers (1982) all have the asymptotic form (4.13). Therefore from (4.3) and (4.5) it is seen that the asymptotic form of the interface shape for $\hat{r} \to \infty$ is

$$\theta = (\theta_w + \dots) + Ca\{f(\theta_w, \lambda) \ln \hat{r} + Q_1^* + \dots\} + \dots, \tag{4.14}$$

where Q_1^* depends on λ, θ_w and the particular slip law which is chosen.

5. Matching with two and three regions

When the parameter ϵ is kept fixed and small while $Ca \to 0$, the expansion (3.26) in Ca valid in the outer region can be matched directly onto the expansion (4.14) in Ca valid in the inner region. This was done by Dussan V. (1976), Huh & Mason (1977*b*) and Hocking (1977) for particular cases. Thus writing (4.14) in outer variables, we obtain

$$\theta = \{\theta_w + \ldots\} + Ca\{f(\theta_w, \lambda)\ln r + f(\theta_w, \lambda)\ln(\epsilon^{-1}) + Q_i^* + \ldots\} + \ldots, \tag{5.1}$$

which must be the form of the outer region expansion for $r \to 0$. Comparing this with (3.28), we obtain

$$\theta_{m0} = \theta_w, \quad \theta_{m1} + Q_0^* = f(\theta_w, \lambda)\ln(\epsilon^{-1}) + Q_i^*, \tag{5.2}$$

so that by (3.27), the value of θ_m is

$$\theta_m = \theta_w + Ca\{f(\theta_w, \lambda)\ln(\epsilon^{-1}) + Q_i^*(\theta_w) - Q_0^*(\theta_w)\} \tag{5.3}$$

where, since $\theta_m \simeq \theta_w, Q_0^*$ may be evaluated at $\theta = \theta_w$ (instead of $\theta = \theta_m$). This relation (5.3) relates the unknown constant θ_m determining the outer region solution, to the spreading velocity U (involved in the definition of Ca) and to the microscopic contact angle θ_w. This angle θ_m, which will be called the *macroscopic* contact angle, is the angle between the static interface shape $f_0 = 0$ as defined in §3 [see paragraphs following (3.8)] and the solid surface in the *outer* region. Or alternatively, θ_m may be considered as being determined by the asymptotic form (3.26) of the interface shape in the outer region as one approaches the contact line.

The result (5.3) can only be expected to be valid in the general double limit of $Ca \to 0$ and $\epsilon \to 0$ if the quantity $(Ca \ln(\epsilon^{-1}))$ also tends to zero in this limiting process since otherwise the term $Ca\, f(\theta_w, \lambda)\ln(\epsilon^{-1})$ appearing in (5.1) would be of order unity (or larger). This would mean that this equation (5.1), which is the inner solution written in outer variables, should be written as

$$\theta = \{\theta_w + f(\theta_w, \lambda)(Ca \ln(\epsilon^{-1})) + \ldots\} + Ca\{f(\theta_w, \lambda)\ln r + Q_i^* + \ldots\} + \ldots \tag{5.4}$$

for matching onto the outer solution. However this would not be a correct procedure since in the inner region the interface is approximately planar with $\theta = \theta_w$ and cannot therefore be valid at distances from the contact line for which $\theta \simeq \theta_w + f(\theta_w, \lambda)(Ca \ln(\epsilon^{-1}))$ as in (5.4). Thus for $Ca \to 0$ and $\epsilon \to 0$ with $(Ca \ln(\epsilon^{-1}))$ of order unity, there is no overlap of the inner and outer regions. Then a third region, called the *intermediate* region of expansion must exist between the inner and outer regions of expansion in order to connect them. It is for this reason that Hocking & Rivers (1982) needed three regions of expansion in considering this type of limit for the special case of a drop spreading on a planar solid surface. In the subsequent discussion we limit ourselves to this situation where $Ca \to 0$ and $\epsilon \to 0$ with $(Ca \ln(\epsilon^{-1}))$ of order unity so that the three regions of expansion are necessary. In order to perform this expansion process we write

$$\eta \equiv Ca \ln(\epsilon^{-1}), \tag{5.5}$$

and make expansions in Ca taking η as a parameter of order unity in magnitude. Then, since

$$\epsilon \equiv \exp(-\eta\, Ca^{-1}), \tag{5.6}$$

it follows that ϵ is exponentially small. Since only terms of order ϵ^0 were in any case included in the expansions in the outer (§3) and inner (§4) regions the results, which were obtained correct to $O(Ca^{+1})$, are still valid without change in this three-region expansion procedure.

6. Intermediate region

In the intermediate region, where we are concerned with values of r which are much larger than ϵ (so that we are outside the inner region) but much smaller than unity (so that we are inside the outer region), we use independent coordinates $(\tilde{x}, \phi)$ where $\tilde{x}$ is defined by†

$$\tilde{x} = Ca \ln \epsilon \hat{r}, \tag{6.1}$$

where as in §4 the origin of the polar coordinates $(\hat{r}, \phi)$ is at the actual contact line and where

$$-\eta < \tilde{x} < 0. \tag{6.2}$$

This region corresponds to that investigated by Pisman & Nir (1982). Since for r small and of order unity, $r \simeq \epsilon \hat{r}$ giving

$$r = \exp(Ca^{-1}\tilde{x}), \tag{6.3}$$

it follows for any fixed value of $\tilde{x}$ in the range (6.2), that r becomes exponentially small as $Ca \rightarrow 0$. Thus for these values of $\tilde{x}$ one is inside the outer region. However the end point $\tilde{x} = 0$ corresponds to the outer region (with r of order unity) so that the intermediate region must be matched onto the outer region at $\tilde{x} = 0$. Similarly, since

$$\hat{r} = \exp\{Ca^{-1}(\tilde{x}+\eta)\}, \tag{6.4}$$

it is seen that $\hat{r}$ becomes exponentially large as $Ca \rightarrow 0$ for $\tilde{x}$ satisfying (6.2). Thus for such values of $\tilde{x}$, one is outside the inner region. However the end-point $\tilde{x} = -\eta$ corresponds to $\hat{r}$ of order unity so that the intermediate region must be matched onto the inner region at $\tilde{x} = -\eta$, this being a negative value of $\tilde{x}$ with magnitude of order unity.

Since, for a fixed value of $\tilde{x}$ in this region, the value of r and hence the value of the curvature of the contact line (of order unity in the outer region) is exponentially small for $Ca \rightarrow 0$, the flow field is, to within such an exponentially small term, two-dimensional so that it may be expressed in terms of a stream function ψ. The velocity field $\boldsymbol{u}$ will be considered as a function of $\tilde{x}$, ϕ and an expansion made in Ca with η taken as a parameter of order unity so that in liquid A

$$\boldsymbol{u}_{\mathrm{A}}(\tilde{x}, \phi; \eta, Ca) = \boldsymbol{u}_{\mathrm{A}0}(\tilde{x}, \phi; \eta) + Ca\, \boldsymbol{u}_{\mathrm{A}1}(\tilde{x}, \phi; \eta) + \dots, \tag{6.5}$$

whilst in a similar manner the liquid–liquid interface shape may be expanded as

$$\phi = \tilde{\beta}(\tilde{x};\, \eta, Ca) \equiv \tilde{\beta}_0(\tilde{x}; \eta) + Ca\, \tilde{\beta}_1(x; \eta) + \dots. \tag{6.6}$$

The stream function ψ and pressure field p corresponding to the flow field (6.5) are then of the form

$$\psi_{\mathrm{A}}(\tilde{x}, \phi; \eta, Ca) = r\tilde{g}_{\mathrm{A}}(\tilde{x}, \phi; \eta, Ca) = r[\tilde{g}_{\mathrm{A}0}(\tilde{x}, \phi; \eta) + Ca\, \tilde{g}_{\mathrm{A}1}(\tilde{x}, \phi; \eta) + \dots], \tag{6.7}$$

$$p_{\mathrm{A}}(\tilde{x}, \phi; \eta, Ca) = r^{-1}\tilde{h}_{\mathrm{A}}(\tilde{x}, \phi; \eta, Ca) = r^{-1}[\tilde{h}_{\mathrm{A}0}(\tilde{x}, \phi; \eta) + Ca\, \tilde{h}_{\mathrm{A}1}(\tilde{x}, \phi; \eta) + \dots]. \tag{6.8}$$

We will use throughout subscripts A and B to refer to quantities pertaining to liquids A and B respectively. Where no suffix is given, the quantity is taken to pertain to either liquid A or liquid B in the equation concerned. The angle θ that the tangent to the liquid–liquid interface given by (6.6) makes with the solid surface [figure 1*b*] is

$$\theta = \tilde{\beta} + \tan^{-1}\left(\mathrm{r}\frac{\mathrm{d}\phi}{\mathrm{d}r}\right) = \tilde{\beta} + \tan^{-1}\left(\mathrm{Ca}\frac{\mathrm{d}\tilde{\beta}}{\mathrm{d}\tilde{x}}\right). \tag{6.9}$$

† This is different (although equivalent) to the independent variable used by Hocking & Rivers (1982).

From the form (6.7) of the stream function, the radial component u_r and transverse component u_ϕ of the velocity field have values in either liquid of the form

$$u_r = \frac{\partial \tilde{g}}{\partial \phi} \quad u_\phi = -\tilde{g} - Ca\frac{\partial \tilde{g}}{\partial \tilde{x}}. \tag{6.10}$$

Since the stream function ψ must satisfy the biharmonic equation, it is found, by direct substitution of the form (6.7) for ψ, that $\tilde{g}(\tilde{x}, \phi)$ must satisfy

$$\left(\frac{\partial^2}{\partial \phi^2}+1\right)^2 \tilde{g} = 2Ca^2\frac{\partial^2}{\partial \tilde{x}^2}\left(1-\frac{\partial^2}{\partial \phi^2}\right)\tilde{g} - Ca^4\frac{\partial^4 \tilde{g}}{\partial \tilde{x}^4}. \tag{6.11}$$

If the expressions (6.8) and (6.10) are substituted into the creeping flow equations (3.1) (or (3.2)) in polar coordinates and the resulting relations put in terms of the intermediate region coordinates, we obtain

$$\tilde{h} = \left(-\frac{\partial \tilde{g}}{\partial \phi}-\frac{\partial^3 \tilde{g}}{\partial \phi^3}\right)+Ca\left(-3\frac{\partial^2 \tilde{g}}{\partial \tilde{x}\,\partial \phi}-\frac{\partial^4 \tilde{g}}{\partial \tilde{x}\,\partial \phi^3}\right)+Ca^2\left(-4\frac{\partial^3 \tilde{g}}{\partial \tilde{x}^2\,\partial \phi}-\frac{\partial^5 \tilde{g}}{\partial \tilde{x}^2\,\partial \phi^3}\right)+\dots. \tag{6.12}$$

At the solid–liquid surfaces $\phi = 0$ and $\phi = \pi$, the boundary condition on u_r, at lowest order, is $u_r = 0$, there being zero error for slip model (i) (see §1) and an error of order $\epsilon^p r^{-p}$ for slip model (iii) (with $p = 1$ for slip model (ii)) since from the form of the flow field, the velocity gradient is proportional to r^{-1} for $r \gg \epsilon$. However from (6.1) and (5.6)

$$\epsilon^p r^{-p} = \exp\{-pCa^{-1}(\tilde{x}+\eta)\},$$

which is exponentially small for $Ca \to 0$ since $\tilde{x} > -\eta$ and $p > 0$. Thus neglecting such terms, the boundary conditions $u_\phi = 0$ and $u_r = 0$ on the solid surface become

$$\tilde{g}_A + Ca\frac{\partial \tilde{g}_A}{\partial \tilde{x}} = 0 \quad \frac{\partial \tilde{g}_A}{\partial \phi} = +1 \quad \text{on } \phi = 0 \tag{6.13}$$

$$\tilde{g}_B + Ca\frac{\partial \tilde{g}_B}{\partial \tilde{x}} = 0 \quad \frac{\partial \tilde{g}_B}{\partial \phi} = -1 \quad \text{on } \phi = \pi. \tag{6.14}$$

The above normal-velocity condition at the solid surface for liquid A may be integrated to give

$$\tilde{g}_A = A\exp(-Ca^{-1}\tilde{x})$$

where A is a constant. This corresponds, as expected, to $\psi = A$. We can choose, without loss of generality, $A = 0$, giving $\tilde{g}_A = 0$. Similarly one can show that $\tilde{g}_B = 0$ on $\phi = \pi$. Thus boundary conditions (6.13) and (6.14) may be written as

$$\tilde{g}_A = 0 \quad \frac{\partial \tilde{g}_A}{\partial \phi} = +1 \quad \text{on } \phi = 0, \tag{6.15}$$

$$\tilde{g}_B = 0 \quad \frac{\partial \tilde{g}_B}{\partial \phi} = -1 \quad \text{on } \phi = \pi. \tag{6.16}$$

Should the interface configuration be time-dependent, then the condition (3.22) for the neglect of this unsteadiness takes the form

$$T \gg \frac{R}{U}\exp(Ca^{-1}\tilde{x}).$$

This is satisfied for all $\tilde{x} < 0$, if (3.23) is satisfied, the effect of stresses resulting from the unsteadiness then being exponentially small as $Ca \to 0$. Thus the normal component of velocity u_n at the interface in the intermediate region may be taken to be zero. However, u_n (for either liquid) is

$$u_n = u_\phi \cos\delta - u_r \sin\delta, \tag{6.17}$$

where $\delta = \theta - \tilde{\beta} = \tan^{-1}(\mathrm{Ca}\, \mathrm{d}\tilde{\beta}/\mathrm{d}\tilde{x})$, is the angle between the radius vector and the tangent to the interface. Substituting this value of δ and the form of the velocity field given by (6.10), into (6.17), we obtain

$$u_n = \left\{1 + \left(Ca\frac{\mathrm{d}\tilde{\beta}}{\mathrm{d}\tilde{x}}\right)^2\right\}^{-\frac{1}{2}} \left\{-1 - Ca\frac{\mathrm{d}}{\mathrm{d}\tilde{x}}\right\}\tilde{g}, \tag{6.18}$$

where

$$\frac{\mathrm{d}}{\mathrm{d}\tilde{x}} \equiv \frac{\partial}{\partial\tilde{x}} + \frac{\mathrm{d}\tilde{\beta}}{\mathrm{d}\tilde{x}}\frac{\partial}{\partial\phi}$$

is the total derivative with respect to $\tilde{x}$ along the interface. By an argument similar to that preceding (6.15), it is seen that the boundary condition $u_n = 0$ reduces to

$$\tilde{g}_{\mathrm{A}} = \tilde{g}_B = 0 \quad \text{on } \phi = \tilde{\beta}, \tag{6.19}$$

which is thus the kinematic boundary condition correct to all orders in Ca. In a similar manner, the exact expression for the tangential component u_t of velocity directed away from the contact line at the interface, is found to be

$$u_t = \left\{1 + \left(Ca\frac{\mathrm{d}\tilde{\beta}}{\mathrm{d}\tilde{x}}\right)^2\right\}^{+\frac{1}{2}} \frac{\partial\tilde{g}}{\partial\phi}, \tag{6.20}$$

where use has been made of the result (6.19). Thus continuity of tangential velocity at the interface implies that

$$\frac{\partial\tilde{g}_{\mathrm{A}}}{\partial\phi} = \frac{\partial\tilde{g}_{\mathrm{B}}}{\partial\phi} \quad \text{on } \phi = \tilde{\beta} \tag{6.21}$$

this being correct to all orders in Ca. The exact expression for the tangential stress τ_t directed away from the contact line and acting on the interface due to the motion of liquid A is

$$\tau_{t\mathrm{A}} = -r^{-1}\left\{1 + \left(Ca\frac{\mathrm{d}\tilde{\beta}}{\partial\tilde{x}}\right)^2\right\}^{-1}\left\{\left(\tilde{g}_{\mathrm{A}} + \frac{\partial^2\tilde{g}_{\mathrm{A}}}{\partial\phi^2}\right) + Ca^2\left(\frac{\mathrm{d}^2\tilde{\beta}}{\partial\tilde{x}^2}\frac{\partial\tilde{g}_{\mathrm{A}}}{\partial\phi} - 2\frac{\mathrm{d}\tilde{\beta}}{\mathrm{d}\tilde{x}}\frac{\partial^2\tilde{g}_{\mathrm{A}}}{\partial\tilde{x}\,\partial\phi}\right) + Ca^4\left(\frac{\mathrm{d}\tilde{\beta}}{\mathrm{d}\tilde{x}}\right)^2\frac{\partial^2\tilde{g}_{\mathrm{A}}}{\partial\tilde{x}^2}\right\}, \tag{6.22}$$

where use is again made of the result (6.19). Thus the continuity of tangential stress becomes

$$\left(\tilde{g}_{\mathrm{A}} + \frac{\partial^2\tilde{g}_{\mathrm{A}}}{\partial\phi^2}\right) - \lambda\left(\tilde{g}_{\mathrm{B}} + \frac{\partial^2\tilde{g}_{\mathrm{B}}}{\partial\phi^2}\right) = O(Ca^2) \quad \text{on } \phi = \tilde{\beta}, \tag{6.23}$$

for $Ca \to 0$. By making use of the expressions (6.8) and (6.12) for the pressure, the normal component of stress that the liquid A exerts on the interface (directed from liquid A to liquid B) is found to be

$$\tau_{n\mathrm{A}} = r^{-1}\left[\left(-\frac{\partial\tilde{g}_{\mathrm{A}}}{\partial\phi} - \frac{\partial^3\tilde{g}_{\mathrm{A}}}{\partial\phi^3}\right) + Ca\left(-\frac{\partial^2\tilde{g}_{\mathrm{A}}}{\partial\tilde{x}\,\partial\phi} - \frac{\partial^4\tilde{g}_{\mathrm{A}}}{\partial\tilde{x}\,\partial\phi^3} + 2\frac{\mathrm{d}\tilde{\beta}}{\mathrm{d}\tilde{x}}\frac{\partial^2\tilde{g}_{\mathrm{A}}}{\partial\phi^2}\right) + Ca^2\left(-4\frac{\partial^3\tilde{g}_{\mathrm{A}}}{\partial\tilde{x}^2\,\partial\phi} - \frac{\partial^5\tilde{g}_{\mathrm{A}}}{\partial\tilde{x}^2\,\partial\phi^3}\right) + \dots\right], \tag{6.24}$$

where use is again made of the result (6.19). The curvature κ of the liquid–liquid interface is

$$\kappa = \cos\delta\frac{\mathrm{d}\theta}{\mathrm{d}r} = Ca\, r^{-1}\cos\delta\frac{\mathrm{d}\theta}{\mathrm{d}x}, \tag{6.25}$$

where $\theta = \tilde{\beta}+\tan^{-1}(Ca(\mathrm{d}\tilde{\beta}/\mathrm{d}x))$ and $\delta = \tan^{-1}(Ca(\mathrm{d}\tilde{\beta}/\mathrm{d}\tilde{x}))$, so that the exact expression for κ is

$$\kappa = Ca\, r^{-1}\left\{1+\left(Ca\frac{\mathrm{d}\tilde{\beta}}{\mathrm{d}\tilde{x}}\right)^2\right\}^{-\frac{3}{2}}\left\{\frac{\mathrm{d}\tilde{\beta}}{\mathrm{d}\tilde{x}}+Ca\frac{\mathrm{d}^2\tilde{\beta}}{\mathrm{d}\tilde{x}^2}+Ca^2\left(\frac{\mathrm{d}\tilde{\beta}}{\mathrm{d}\tilde{x}}\right)^3\right\}. \tag{6.26}$$

The normal-stress boundary condition $\kappa = +Ca(\tau_{n\mathrm{B}}-\tau_{n\mathrm{A}})$ may therefore be expressed as

$$\begin{aligned}\frac{\mathrm{d}\tilde{\beta}}{\mathrm{d}\tilde{x}}+Ca\frac{\mathrm{d}^2\tilde{\beta}}{\mathrm{d}\tilde{x}^2} = &\left\{\left(\frac{\partial\tilde{g}_\mathrm{A}}{\partial\phi}+\frac{\partial^3\tilde{g}_\mathrm{A}}{\partial\phi^3}\right)-\lambda\left(\frac{\partial\tilde{g}_\mathrm{B}}{\partial\phi}+\frac{\partial^3\tilde{g}_\mathrm{A}}{\partial\phi^3}\right)\right\}+Ca\left\{\left(\frac{\partial^2\tilde{g}_\mathrm{A}}{\partial\tilde{x}\,\partial\phi}+\frac{\partial^4\tilde{g}_\mathrm{A}}{\partial\tilde{x}\,\partial\phi^3}-2\frac{\mathrm{d}\tilde{\beta}}{\mathrm{d}\tilde{x}}\frac{\partial^2\tilde{g}_\mathrm{A}}{\partial\phi^2}\right)\right.\\ &\left.-\lambda\left(\frac{\partial^2\tilde{g}_\mathrm{B}}{\partial\tilde{x}\,\partial\phi}+\frac{\partial^4\tilde{g}_\mathrm{B}}{\partial\tilde{x}\,\partial\phi^3}-2\frac{\mathrm{d}\tilde{\beta}}{\mathrm{d}\tilde{x}}\frac{\partial^2\tilde{g}_\mathrm{B}}{\partial\phi^2}\right)\right\}+O(Ca^2),\end{aligned} \tag{6.27}$$

where the right-hand side is evaluated at $\phi = \tilde{\beta}$. By operating on (6.27) with $(1-Ca(\mathrm{d}/\mathrm{d}\tilde{x})$ and making use of (6.11) and (6.19), we obtain

$$\frac{\mathrm{d}\tilde{\beta}}{\mathrm{d}\tilde{x}} = \left[\left(\frac{\partial\tilde{g}_\mathrm{A}}{\partial\phi}+\frac{\partial^3\tilde{g}_\mathrm{A}}{\partial\phi^3}\right)-\lambda\left(\frac{\partial\tilde{g}_\mathrm{B}}{\partial\phi}+\frac{\partial^3\tilde{g}_\mathrm{B}}{\partial\phi^3}\right)\right]\left[1-Ca\left(\frac{\partial^2\tilde{g}_\mathrm{A}}{\partial\phi^2}-\lambda\frac{\partial^2\tilde{g}_\mathrm{B}}{\partial\phi^2}\right)\right]+O(Ca)^2 \tag{6.28}$$

which by the use of (6.19) and (6.23) further reduces to

$$\frac{\mathrm{d}\tilde{\beta}}{\mathrm{d}\tilde{x}} = \left\{\left(\frac{\partial\tilde{g}_\mathrm{A}}{\partial\phi}+\frac{\partial^3\tilde{g}_\mathrm{A}}{\partial\phi^3}\right)-\lambda\left(\frac{\partial\tilde{g}_\mathrm{B}}{\partial\phi}+\frac{\partial^3\tilde{g}_\mathrm{B}}{\partial\phi^3}\right)\right\}+O(Ca)^2, \tag{6.29}$$

the right-hand side of which is evaluated at $\phi = \tilde{\beta}$. It should be noted that a static pressure drop (of order $Ca^{-1}\Delta P$ in outer variables) would give rise to a term $r^{+1}\Delta P \equiv \Delta P\exp(Ca^{-1}\tilde{x})$ in (6.26). This may be neglected since it is exponentially small as $Ca\to 0$ for any fixed value of $\tilde{x}$ in the intermediate region. Also note that in our present problem no terms of order Ca^{+1} appear in the differential equation (6.11) or in the boundary conditions (6.15), (6.16), (6.19), (6.21), (6.23) and (6.29), despite the fact that a term of order Ca^{+1} occurs in the expression for the pressure.

7. General solution

The expansions (6.7) and (6.6) for $\tilde{g}_\mathrm{A}$, $\tilde{g}_\mathrm{B}$ and $\tilde{\beta}$ valid for small Ca must be of the form

$$\left.\begin{aligned}\tilde{g}_\mathrm{A} = \tilde{g}_{\mathrm{A}0}+Ca^2\tilde{g}_{\mathrm{A}2}+\ldots,\quad \tilde{g}_\mathrm{B} = \tilde{g}_{\mathrm{B}0}+Ca^2\tilde{g}_{\mathrm{B}2}+\ldots,\\ \tilde{\beta} = \tilde{\beta}_0+Ca^2\tilde{\beta}_2+\ldots,\end{aligned}\right\} \tag{7.1}$$

since, as noted above, the equations and boundary conditions for these variables contain no term in Ca^{+1}. Then $\tilde{g}_{\mathrm{A}0}$ and $\tilde{g}_{\mathrm{B}0}$ satisfy

$$\left(\frac{\partial^2}{\partial\phi^2}+1\right)^2\tilde{g}_0 = 0, \tag{7.2}$$

in either liquid, with

$$\tilde{g}_{A0} = 0, \quad \frac{\partial \tilde{g}_{A0}}{\partial \phi} = +1, \quad \text{on } \phi = 0, \tag{7.3}$$

$$\tilde{g}_{B0} = 0, \quad \frac{\partial \tilde{g}_{B0}}{\partial \phi} = -1, \quad \text{on } \phi = \pi, \tag{7.4}$$

$$\tilde{g}_{A0} = \tilde{g}_{B0} = 0 \quad \text{on } \phi = \tilde{\beta}_0, \tag{7.5}$$

$$\frac{\partial \tilde{g}_{A0}}{\partial \phi} = \frac{\partial \tilde{g}_{B0}}{\partial \phi} \quad \text{on } \phi = \tilde{\beta}_0, \tag{7.6}$$

$$\left(\tilde{g}_{A0} + \frac{\partial \tilde{g}_{A0}}{\partial \phi^2}\right) = \lambda \left(\tilde{g}_{B0} + \frac{\partial^2 \tilde{g}_{B0}}{\partial \phi^2}\right) \quad \text{on } \phi = \tilde{\beta}_0, \tag{7.7}$$

It is observed that this set of equations and boundary conditions are identical with those for flow assuming a planar liquid–liquid interface (see (3.11)–(3.16)). Hence as in §3,

$$\left.\begin{aligned} \tilde{g}_{A0} &= (C_A \phi + D_A) \cos\phi + (E_A \phi + F_A) \sin\phi, \\ \tilde{g}_{B0} &= (C_B \phi + D_B) \cos\phi + (E_B \phi + F_B) \sin\phi, \end{aligned}\right\} \tag{7.8}$$

where $C_A, D_A \ldots$ are given by (3.18) and (3.19) with $\tilde{\beta}_0$ replacing θ_m. Then by substituting the expansion (7.1) for $\tilde{\beta}$ into the normal stress boundary condition (6.29), we obtain

$$\frac{d\tilde{\beta}_0}{d\tilde{x}} = f(\tilde{\beta}_0), \tag{7.9}$$

where the function $f(\tilde{\beta})$ is given by (3.21). Thus

$$g(\tilde{\beta}_0, \lambda) + K = \tilde{x}, \tag{7.10}$$

where

$$g(\tilde{\beta}, \lambda) = \int_0^{\tilde{\beta}} \frac{d\beta}{f(\beta, \lambda)}, \tag{7.11}$$

and K is a constant of integration. Since the slope angle θ of the interface is given by (6.9) and hence by

$$\theta = \tilde{\beta}_0 + Ca \frac{d\tilde{\beta}_0}{d\tilde{x}} + O(Ca^2), \tag{7.12}$$

the interface shape (7.10) in the intermediate region may be written alternatively as

$$g(\theta, \lambda) = -K + \tilde{x} + Ca + O(Ca^2). \tag{7.13}$$

If the asymptotic form (3.26) of the solution in the outer region is written in terms of intermediate variables it is seen that for matching we require that

$$g(\theta, \lambda) \sim g(\theta_m, \lambda) + Ca \frac{Q_0^*}{f(\theta_m, \lambda)} + \tilde{x} \quad \text{as } \tilde{x} \to 0. \tag{7.14}$$

Thus for matching of terms at orders Ca^0 and Ca^{+1} we require

$$-K + Ca = g(\theta_m, \lambda) + Ca \frac{Q_0^*}{f(\theta_m, \lambda)}, \tag{7.15}$$

with the terms of order $\tilde{x}$ in (7.13) and (7.14) automatically matching. If we write

$$\tilde{x} = -\eta + \tilde{y}, \tag{7.16}$$

so that $\tilde{y}\to 0$ in the intermediate region where we require matching onto the inner-region expansion, then the intermediate-region solution is

$$g(\theta,\lambda) = (-K-\eta)+\tilde{y}+Ca+O(Ca^2), \tag{7.17}$$

whilst the asymptotic form (4.14) of the inner solution for $\hat{r}\to\infty$, may be written in terms of $\tilde{y}$ to obtain for matching that

$$g(\theta,\lambda) \sim g(\theta_{\mathrm{w}},\lambda)+Ca\frac{Q_{\mathrm{i}}^*}{f(\theta_{\mathrm{w}},\lambda)}+\tilde{y} \quad \text{as } \tilde{y}\to 0. \tag{7.18}$$

Thus for matching of terms at orders Ca^0 and Ca^{+1} we require

$$-K-\eta+Ca = g(\theta_{\mathrm{w}},\lambda)+Ca\frac{Q_{\mathrm{i}}^*}{f(\theta_{\mathrm{w}},\lambda)}, \tag{7.19}$$

with the terms of order $\tilde{y}$ in (7.17) and (7.18) automatically matching. The elimination of K from (7.15) and (7.19) yields

$$g(\theta_{\mathrm{m}}) = \{g(\theta_{\mathrm{w}})+\mathrm{Ca}\ln(\epsilon^{-1})\}+Ca\{(f(\theta_{\mathrm{w}}))^{-1}Q_{\mathrm{i}}^*-(f(\theta_{\mathrm{m}}))^{-1}Q_0^*\}+O(Ca^2), \tag{7.20}$$

for the value of the macroscopic contact angle θ_{m} in terms of the spreading velocity correct to order Ca^{+1}. This relation (7.20) may be expressed in the alternative form

$$Ca = \frac{g(\theta_{\mathrm{m}})-g(\theta_{\mathrm{w}})}{\ln(\epsilon^{-1})-(f(\theta_{\mathrm{m}}))^{-1}Q_0^*+(f(\theta_{\mathrm{w}}))^{-1}Q_0^*}+O\left(\frac{1}{\ln(\epsilon^{-1})}\right)^3, \tag{7.21}$$

where use has been made of the assumption that $Ca\ln(\epsilon^{-1})$ is of order unity. This equation is identical to that given by Hocking & Rivers (1982) when applied to the particular problem that they considered. Should the liquid A be receding rather than advancing so that $U<0$, it may readily be seen that the above relations (7.20) and (7.21) are still valid if $Ca\equiv\mu_{\mathrm{A}}U/\sigma$ is taken as negative. The constants Q_0^* and Q_{i}^* are then still defined as in (3.26) and (4.14) respectively (but with Ca now being negative).

The result (7.20) correct to order Ca^0 gives the zeroth-order value $\theta_{\mathrm{m}0}$ of the macroscopic contact angle as

$$g(\theta_{\mathrm{m}0}) = g(\theta_{\mathrm{w}})+Ca\ln(\epsilon^{-1}). \tag{7.22}$$

The solution correct to order Ca^{+1} for any particular problem may be obtained as follows. For any given position of the contact line, the solution in the outer region at order Ca^0 (i.e. the static configuration) would determine the value of $\theta_{\mathrm{m}0}$ (i.e. the macroscopic contact angle at order Ca^0) at all positions along the contact line. The above relation (7.22) applied at each position on the contact line would then give the approximate spreading velocity U (correct to order $(\sigma/\mu_{\mathrm{A}})(\ln(\epsilon^{-1}))^{-1}$). This may be used to determine the solution in the outer expansion correct to order Ca^{+1} which when compared with the asymptotic form (3.28) at the contact line would determine $\theta_{\mathrm{m}1}$. Equation (7.21) may then be used to determine a more accurate spreading velocity U (correct to order $(\sigma/\mu_{\mathrm{A}}(\ln(\epsilon^{-1}))^{-2})$. This value of U calculated at each position along the contact line can then be used to determine the configuration of the contact line at a slightly later time. In this manner, one can progress forward in time by examining the development in each small time interval. Thus in order to find the motion of the system correct to order Ca^{+1}, we solve simultaneously the equation (7.21) (or (7.20)) correct to order Ca^{+1} with an equation obtained from the outer solution relating θ_{m} to the contact-line position. To be consistent, this latter equation must be used in a form correct to order Ca^{+1}.

8. Discussion

As expected, it is observed that the result (7.20) obtained from the triple-region expansion reduces to the result (5.3) obtained from the double-region expansion when conditions are such that the latter is valid (i.e. $Ca \ln(\epsilon^{-1}) \to 0$ as $Ca \to 0$, $\epsilon \to 0$). However, the two results are distinct when $Ca \ln(\epsilon^{-1})$ is of order unity with (5.3) no longer being valid.

The very simple result (7.22) is very attractive in that it relates the value θ_{m0} of the macroscopic contact angle θ_m correct to order Ca^0 directly to the spreading velocity U through the definition (2.2*a*) of the capillary number with $g(\theta)$ given by (3.21) and (7.11). In order to use (7.22), it is not necessary to calculate the details of the macroscopic flow in the outer region or necessary to know the precise type of slip (or other mechanism) that occurs very close to the contact line. However (7.22) has the disadvantage that the quantity ϵ is not uniquely defined in that it is the ratio of the slip length s to macroscopic lengthscale R where neither length is a unique quantity. The addition of the term of order Ca^{+1} as in (7.20), gets rid of this difficulty. The value of the macroscopic contact angle θ_m at order Ca^0 as given by (7.22) may, in any experiment, be interpreted as the contact angle calculated from macroscopic measurements of the liquid–liquid interface assuming a static interface shape. Thus in any given experiment, such as the movement of a meniscus along a circular tube, the angle θ_m may be interpreted in any number of ways being calculated from, for example, the apex height of the meniscus, the mean radius of curvature of the meniscus or the additional pressure drop due to the meniscus (Hoffman 1975; Kafka & Dussan V. 1979; Ngan & Dussan V. 1982). The values of θ_m determined by these various methods would differ from one another only by an amount of order Ca^{+1}. However the value of θ_m at order Ca^{+1} given by the more accurate result (7.21) must be interpreted more carefully as either (i) the contact angle calculated from the static interface shape with the contact line which actually exists in the outer region or (ii) that determined by the asymptotic form (3.26) of the slope angle θ in the outer region as the contact line is approached. The microscopic contact angle θ_w appearing in (7.21) and (7.22) is the contact angle determined by intermolecular forces acting at the contact line and is assumed to have a unique value, there being no contact-angle hysteresis. For real solid surfaces, however, contact-angle hysteresis does occur and is due, at least in part, to roughness and chemical heterogeneity of the surface (Johnson & Dettre 1964; Cox 1983; Jansons 1985). For such surfaces it is not clear whether θ_w should be taken as that determined by Wenzel's (1936) result for a rough surface or as the static advancing contact angle (for $U > 0$) or possibly as some other value. This question requires further investigation although it would seem reasonable to take θ_w as the static advancing contact angle since from (7.21), $\theta_m \to \theta_w$ as $U \to 0$.

Since one liquid is receding while the other is advancing, the relationships (7.21) (and (7.22)) between contact angle and contact-line speed should be invariant upon interchanging the roles of liquid A and liquid B. Such a transformation may be written as

$$\left.\begin{array}{ll} U \to -U, & \lambda \to \lambda^{-1}, \\ \theta_w \to \pi - \theta_w, & \theta_m \to \pi - \theta_m, \\ Ca \to -\lambda Ca, & \end{array}\right\} \tag{8.1}$$

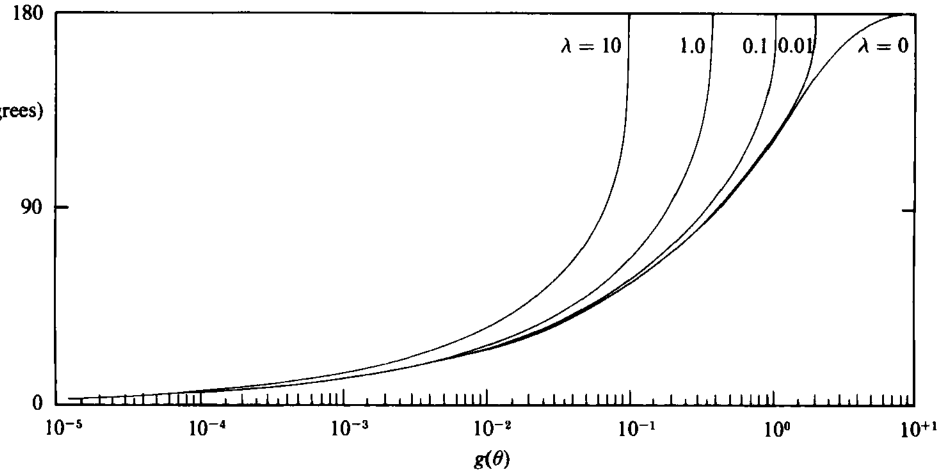

FIGURE 2. $g(\theta)$ for various values of λ.

and it may be verified by direct substitution that this does indeed leave (7.21) (and (7.22)) unchanged if use is made of the results:

$$\left.\begin{aligned} f(\pi-\theta,\lambda^{-1}) &= \lambda^{-1}f(\theta,\lambda) && \text{[obtained from (3.21)]},\\ g(\pi-\theta,\lambda^{-1}) &= \lambda g(\pi,\lambda)-\lambda g(\theta,\lambda) && \text{[obtained from (7.11)]},\\ Q_0^*(\pi-\theta,\lambda^{-1},\ldots) &= \lambda^{-1}Q_0^*(\theta,\lambda,\ldots) && \text{[obtained from (3.26)]},\\ Q_1^*(\pi-\theta,\lambda^{-1},\ldots) &= \lambda^{-1}Q_1^*(\theta,\lambda,\ldots) && \text{[obtained from (4.14)]}.\end{aligned}\right\} \quad (8.2)$$

Since the macroscopic contact angle θ_m depends on ϵ (as seen from (7.20) or (7.22)), it means that by merely changing the macroscopic lengthscale R, keeping all other quantities fixed, the value of θ_m should be altered. That this is so has been demonstrated experimentally by Ngan & Dussan V. (1982) who examined the motion of a meniscus between parallel plates and showed that θ_m was indeed dependent on the separation distance between the plates. In figure 2, graphs are drawn with $g(\theta)$ plotted along the abscissa and θ along the ordinate for various values of the viscosity ratio λ. For any microscopic contact angle θ_w, the value of $g(\theta_w)$ may be read off on the abscissa. Then from (7.22) it is seen that by moving along the abscissa a distance of $(Ca \ln(\epsilon^{-1}))$ to the right if $U > 0$ (or to the left if $U < 0$) the value of θ_m may be read off on the ordinate. It is interesting to note that Hoffman (1975) from his experimental results for a number of liquids with a meniscus advancing along a capillary tube (with $\lambda = 0$) in fact observed that, with such a graphical interpretation, all his results fell on a single line (corresponding to our function $g(\theta)$). In figure 3, lines corresponding to Hoffman's results have been drawn (broken lines) assuming various values of ϵ. If these are compared with the function $g(\theta)$) for $\lambda = 0$ (continuous line), it is seen that good agreement is obtained for all values of θ (except for θ very close to 180°) for a value of $\epsilon = 10^{-4}$. Since in Hoffman's experiments the macroscopic lengthscale (the capillary tube radius) was of the order of 0.1 cm, this would mean a slip length s of 10^{-5} cm. This is very close to the value obtained by Hocking & Rivers (1982) for the very different system they examined, namely the spreading of a molten glass drop on a planar platinum surface. The fact that good agreement is obtained between Hoffman's results and the calculated function $g(\theta)$ for all values of θ suggests that the microscopic contact angle θ_w is, at least for the systems examined, a constant independent of the spreading velocity. The disagree-

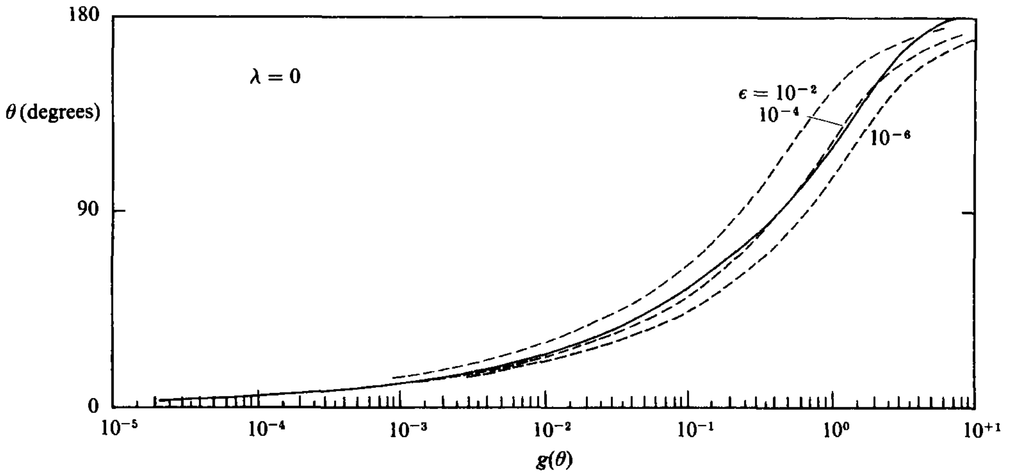

FIGURE 3. $g(\theta)$ from Hoffman's (1975) experimental results taking $\epsilon = 10^{-2}$, 10^{-4} and 10^{-6} (broken lines) and the theoretical value of $g(\theta)$ for $\lambda = 0$ (continuous line).

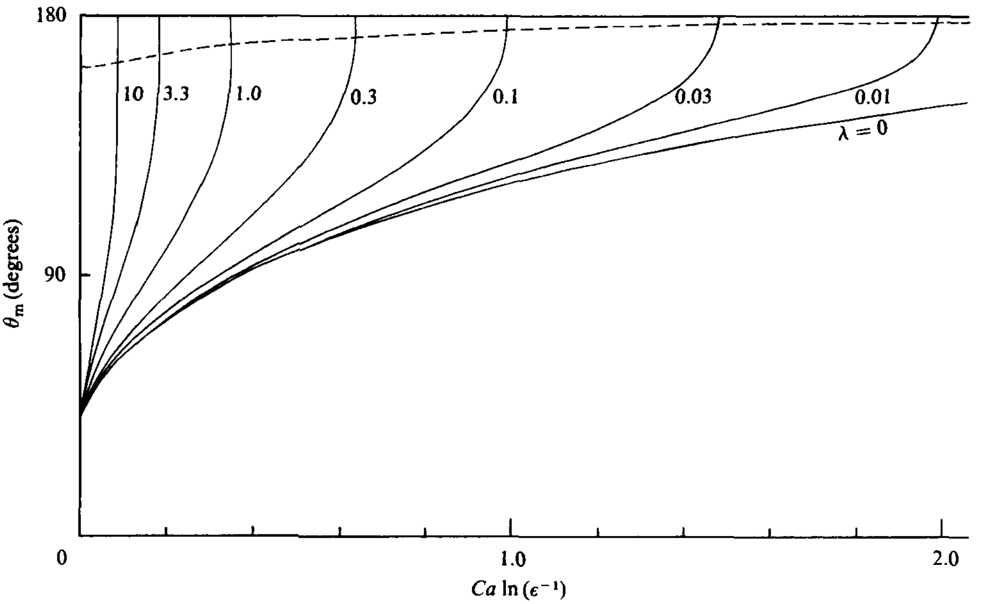

FIGURE 4. Macroscope contact angle θ_m as a function of $(Ca \ln(\epsilon^{-1}))$ for various values of λ with $\theta_w = 40°$. Broken line represents the limit of validity of the theory as determined from (8.11 *b*) with $\epsilon = 10^{-5}$.

ment between the experiment and the theory for values of θ close to 180° may be due to the fact that such values of θ_m corresponded in the experiments to values of the capillary number Ca which were no longer small compared with unity. The values of θ_m as derived from (7.22) are plotted as a function of $(Ca \ln(\epsilon^{-1}))$ for liquid A advancing ($U > 0$) and for various values of λ in figure 4 for the specific case $\theta_w = 40°$. It is observed that for all values of λ except $\lambda = 0$ there is a maximum value of $(Ca \ln(\epsilon^{-1}))$ and hence a maximum spreading velocity U, for which a solution exists, the value of θ_m attaining a value of 180° at this limit. The only situation in which

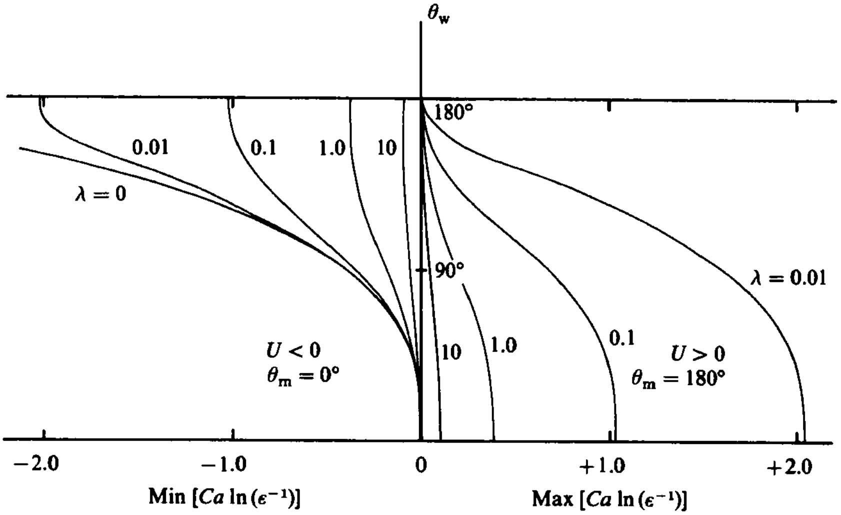

FIGURE 5. Maximum (for $U > 0$) and minimum (for $U < 0$) values of ($Ca \ln(\epsilon^{-1})$) for which a steady solution exists plotted as a function of the microscopic contact angle θ_w for various values of λ.

a solution exists for all U, however large, is the case of the advancing contact line with $\lambda = 0$ (or the equivalent situation of a receding contact line with $\lambda = \infty$). At lowest order, this maximum value Ca_{max} of the capillary number Ca (with $U > 0$) is determined from (7.22) as

$$Ca_{max} = \frac{g(\pi, \lambda) - g(\theta_w, \lambda)}{\ln(\epsilon^{-1})} + O(\ln \epsilon^{-1})^{-2}, \tag{8.3}$$

whilst in a similar manner the minimum value Ca_{min} (for $U < 0$) is found to be

$$Ca_{min} = -\frac{g(\theta_w, \lambda)}{\ln(\epsilon^{-1})} + O(\ln \epsilon^{-1})^{-2}. \tag{8.4}$$

From the value of $g(\theta, \lambda)$ given by (7.11) and (3.21) it may be seen that Ca_{max} does indeed tend to ∞ as $\lambda \to 0$. In fact it may be shown after considerable calculation that the asymptotic form of $g(\pi, \lambda)$ for $\lambda \to 0$ is

$$g(\pi, \lambda) \sim \tfrac{1}{6}\pi \ln\left(\frac{4}{3\pi\lambda}\right) + O(\lambda), \tag{8.5}$$

so that for small λ,

$$Ca_{max} = \frac{\tfrac{1}{6}\pi \ln\left(\frac{4}{3\pi\lambda}\right) - g(\theta_w) + O(\lambda)}{\ln(\epsilon^{-1})} + O(\ln \epsilon^{-1})^{-2}. \tag{8.6}$$

In figure 5 the limiting values of ($Ca \ln(\epsilon^{-1})$) for a solution to exist are shown as a function of θ_w for various values of λ. If, in any particular situation, the spreading velocity is forced to exceed its maximum value, it is speculated that no steady interface shape is possible and that the liquid ahead of the contact line becomes entrained as a film beneath the other liquid behind the contact line. In fact this phenomenon has been observed by Inverarity (1969), Burley & Brady (1973), Burley & Kennedy (1976) and Kennedy & Burley (1977).

Should the results obtained be applied to a situation where the interface configuration is time dependent then for validity we require that (3.23) be satisfied. Thus the theory cannot be applied to (i) the initial stage of spreading of a drop placed on a plane solid surface for which the initial value of the contact angle differs from θ_w or (ii) where, during spreading, the value of θ_w suddenly changes due to, for example, a sudden change in the nature of the solid surface. In each of these situations the characteristic time T is essentially zero.

In addition to the conditions for the validity of the theory already stated (namely that $Ca \to 0$ and $\epsilon \to 0$ with $Ca\,(\ln(\epsilon^{-1}))$ of order unity), an inspection of the values in the intermediate region of τ_t and κ given by (6.22) and (6.26) respectively reveals a further necessary condition that $Ca(d\tilde{\beta}/d\tilde{x}) \ll 1$. Thus, from (7.9) it is seen that we require

$$Caf(\tilde{\beta}) \ll 1 \quad \text{for all } \tilde{\beta} \text{ between } \theta_w \text{ and } \theta_m. \tag{8.7}$$

This is satisfied automatically except for θ_w and/or θ_m lying close to either 0° or 180° since for these values of $\tilde{\beta}$, $f(\tilde{\beta})$ is unbounded with

$$f(\tilde{\beta}) \sim 3\tilde{\beta}^{-2} \quad \text{as } \tilde{\beta} \to 0, \tag{8.8}$$

and

$$f(\tilde{\beta}) \sim 3\lambda(\pi - \tilde{\beta})^{-2} \quad \text{as } \tilde{\beta} \to \pi. \tag{8.9}$$

Thus for the theory to be valid, θ_w and θ_m must be such that

$$\theta_w \gg Ca^{\frac{1}{2}}, \quad \theta_m \gg Ca^{\frac{1}{2}}, \tag{8.10a, b}$$

$$(\pi - \theta_w) \gg (Ca\lambda)^{\frac{1}{2}}, \quad (\pi - \theta_m) \gg (Ca\lambda)^{\frac{1}{2}}. \tag{8.11a, b}$$

The limiting values of θ_m given by (8.11*b*) are indicated in figure 4 for the particular example considered with $\epsilon = 10^{-5}$. Note that this condition imposes no restriction on the value of θ_m for the case $\lambda = 0$. It should also be mentioned that for $\lambda \neq 0$, since the theory does not apply when θ_m gets too close to 180°, there is a problem concerning the validity of the conclusion already stated that there exists a maximum value of spreading velocity U for such situations. This is a question requiring further study.

If, in the intermediate region, the calculated value of $\tilde{g}$ is substituted into (6.20), the tangential component u_t of velocity away from the contact line on the liquid–liquid interface is found to be

$$u_t = \frac{\lambda(\tilde{\beta}^2 - \sin^2\tilde{\beta})\{\sin\tilde{\beta} + (\pi - \tilde{\beta})\cos\tilde{\beta}\} + \{(\pi - \tilde{\beta})^2 - \sin^2\tilde{\beta}\}(\tilde{\beta}\cos\tilde{\beta} - \sin\tilde{\beta})}{\lambda(\tilde{\beta}^2 - \sin^2\tilde{\beta})\{(\pi - \tilde{\beta}) + \sin\tilde{\beta}\cos\tilde{\beta}\} + \{(\pi - \tilde{\beta})^2 - \sin^2\tilde{\beta}\}(\tilde{\beta} - \sin\tilde{\beta}\cos\tilde{\beta})} + O(Ca^2). \tag{8.12}$$

This is plotted as a function of $\tilde{\beta}$ for various values of λ in figure 6 from which it is observed that except for $\lambda = 0$ (or $\lambda = \infty$), u_t changes from negative values (with $u_t = -0.5$ at $\tilde{\beta} = 0$) to positive values (with $u_t = +0.5$ at $\tilde{\beta} = \pi$) as $\tilde{\beta}$ is increased. In fact $u_t = 0$ for $\tilde{\beta} = \tilde{\beta}^*$ where $\tilde{\beta}^*$ satisfies

$$\lambda = \frac{\{(\pi - \tilde{\beta}^*)^2 - \sin^2\tilde{\beta}^*\}(\sin\tilde{\beta}^* - \tilde{\beta}^*\cos\tilde{\beta}^*)}{(\tilde{\beta}^{*2} - \sin^2\tilde{\beta}^*)\{\sin\tilde{\beta}^* + (\pi - \tilde{\beta})\cos\tilde{\beta}^*\}}. \tag{8.13}$$

Since $\tilde{\beta}$ monotonically increases (for $U > 0$) or monotonically decreases (for $U < 0$) as one moves out along the interface away from the contact line in the intermediate region, it is seen that the following three situations are possible: (i) u_t is positive along the entire interface (if $\theta_w, \theta_m < \tilde{\beta}^*$ for $U > 0$); (ii) u_t is negative along the entire interface (if $\theta_w, \theta_m > \tilde{\beta}^*$ for $U > 0$); (iii) u_t is negative close to the contact line but

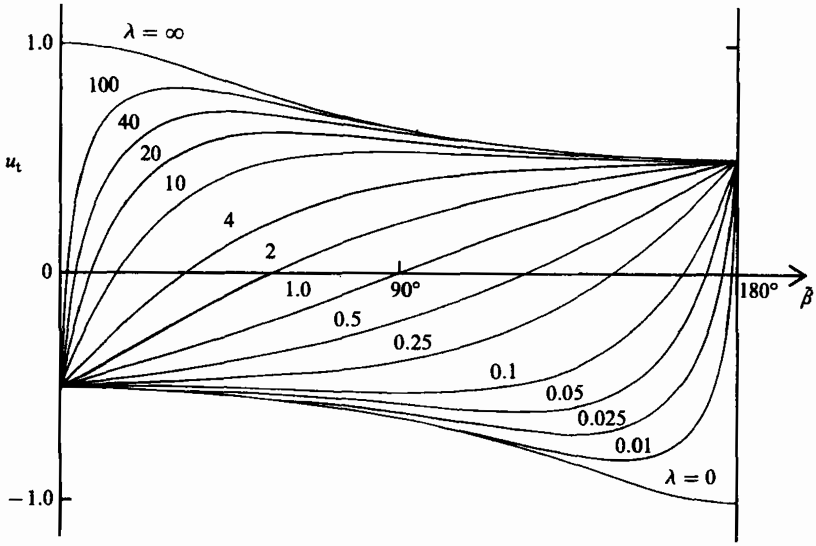

FIGURE 6. Tangential component of velocity u_t directed away from the contact line as a function of $\tilde{\beta}$ for various values of λ.

positive farther from the contact line (if $\theta_w < \tilde{\beta}^* < \theta_m$ for $U > 0$) with u_t changing sign at $\tilde{\beta} = \tilde{\beta}^*$. The type of interface flow present is of importance concerning the transport and hence the effect of any surfactant which may be present.

In addition to being zero on the solid boundary and on the liquid–liquid interface, the stream function ψ in the intermediate region is also zero where either $\tilde{g}_A$ or $\tilde{g}_B$ is zero. This occurs where ϕ satisfies

$$\left.\begin{aligned}\tan\phi &= -\frac{C_A(\tilde{\beta})\,\phi + D_A(\tilde{\beta})}{E_A(\tilde{\beta})\,\phi + F_A(\tilde{\beta})},\\ &= \frac{\sin\tilde{\beta}[\lambda\{\pi\sin\tilde{\beta} + \sin^2\tilde{\beta}\cos\tilde{\beta} + \tilde{\beta}(\pi-\tilde{\beta})\cos\tilde{\beta}\} + \cos\tilde{\beta}\{(\pi-\tilde{\beta})^2 - \sin^2\tilde{\beta}\}]\,\phi}{\sin^2\tilde{\beta}[-\lambda\{\sin^2\tilde{\beta} + \tilde{\beta}(\pi-\tilde{\beta})\} - \{(\pi-\tilde{\beta})^2 - \sin^2\tilde{\beta}\}]\,\phi \\ \qquad + \tilde{\beta}[\lambda\{\sin^2\tilde{\beta} + \tilde{\beta}(\pi-\tilde{\beta}) + \pi\sin\tilde{\beta}\cos\tilde{\beta}\} + \{(\pi-\tilde{\beta})^2 - \sin^2\tilde{\beta}\}]},\end{aligned}\right\} \tag{8.14}$$

with $0 \leqslant \phi \leqslant \tilde{\beta}$ (i.e. in liquid A) or where ϕ satisfies

$$\left.\begin{aligned}\tan\phi &= -\frac{C_B(\tilde{\beta})\,\phi + D_B(\tilde{\beta})}{E_B(\tilde{\beta})\,\phi + F_B(\tilde{\beta})},\\ &= \frac{\sin\tilde{\beta}[-\lambda\cos\tilde{\beta}(\tilde{\beta}^2 - \sin^2\tilde{\beta}) + \{+\pi\sin\tilde{\beta} - \sin^2\tilde{\beta}\cos\tilde{\beta} - \tilde{\beta}(\pi-\tilde{\beta})\cos\tilde{\beta}\}](\pi-\phi)}{\sin^2\tilde{\beta}[\lambda(\tilde{\beta}^2 - \sin^2\tilde{\beta}) + \{\sin^2\tilde{\beta} + \tilde{\beta}(\pi-\tilde{\beta})\}](\pi-\phi) \\ \qquad - (\pi-\tilde{\beta})[\lambda(\tilde{\beta}^2 - \sin^2\tilde{\beta}) + \{\sin^2\tilde{\beta} + \tilde{\beta}(\pi-\tilde{\beta}) - \pi\sin\tilde{\beta}\cos\tilde{\beta}\}]},\end{aligned}\right\} \tag{8.15}$$

with $\tilde{\beta} \leqslant \phi \leqslant \pi$ (i.e. in liquid B). These values of ϕ have been plotted as a function of $\tilde{\beta}$ for various values of λ in figure 7, from which it is observed that for any given value of $\tilde{\beta}$ (and λ), these equations (8.14) and (8.15) taken together possess exactly one solution for ϕ. Thus if in these equations the interface shape $\tilde{\beta} = \tilde{\beta}(\tilde{x})$ is substituted, it is seen that the resulting value of ϕ considered as a function of $\tilde{x}$

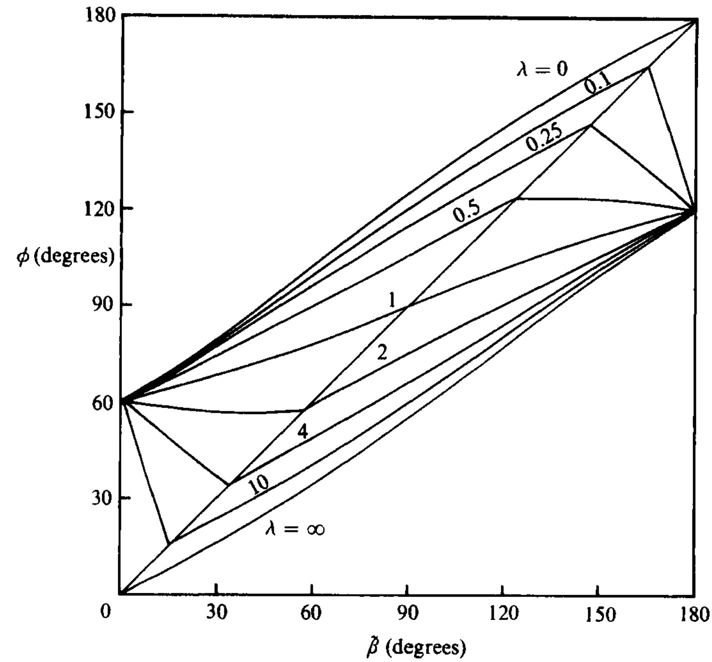

FIGURE 7. Values of ϕ as a function of $\tilde{\beta}$ (for various values of λ) for the streamline passing through the contact line.

represents a streamline passing through the contact line. It is also noted from figure 7 that for any fixed value of $\lambda (\lambda \neq 0$ and $\lambda \neq \infty)$ that when $\tilde{\beta} = 0$, $\phi = \frac{1}{3}\pi$ and that as $\tilde{\beta}$ increases from zero, ϕ is initially greater than $\tilde{\beta}$ (so that the streamline is in liquid B) but that at a critical value of $\tilde{\beta}$ ($= \tilde{\beta}^*$ where $\tilde{\beta}^*$ is given by (8.13)), $\phi = \tilde{\beta}$ so that the streamline meets the liquid–liquid interface. For larger values of $\tilde{\beta}$, the angle ϕ is less than $\tilde{\beta}$ (so that the streamline is in liquid A) with $\phi \rightarrow \frac{2}{3}\pi$ as $\tilde{\beta} \rightarrow \pi$. From these results sketches have been drawn (figure 8) of the form of the streamlines in the intermediate region for each of the three cases (i), (ii) and (iii) mentioned above. It is interesting to note that for the case (iii) there is a vortex ahead of an advancing liquid–liquid interface. This vortex is different from the one reported by Dussan, V. (1977, 1979) which was present in the *outer* region for the particular case of the motion of a meniscus along a capillary tube.

From (6.8) and (6.11), it is seen that the pressure due to the flow in the intermediate region in liquid A at the solid surface $\phi = 0$ is $2r^{-1}C_A$ (and in liquid B at $\phi = \pi$ is $-2\lambda r^{-1}C_B$). This has been plotted as a function of $\tilde{\beta}$ for various values of λ in figure 9 from which it is observed that for λ greater than a critical value (0.148) the pressure is negative on the solid surface behind an advancing contact line but if λ is less than this value, positive or negative values of the pressure can occur behind the advancing contact line depending on the value of $\tilde{\beta}$. At a distance r from the contact line, the dimensional pressure is of order $\mu_A U r^{-1}$ which for values of spreading velocity U for which $Ca \ln(\epsilon^{-1}) = O(1)$ gives a value of order $\sigma r^{-1}(\ln(\epsilon^{-1}))^{-1}$ which can be of order one atmosphere or more for r in the range 10^{-6} to 10^{-4} cm. This indicates that in the regions where p is negative that at these distances from the contact line, cavitation might possibly take place. In this connection, the minimum value of the pressure p due to the flow (for $p < 0$) occurring for any ϕ in either liquid is plotted in figure 10

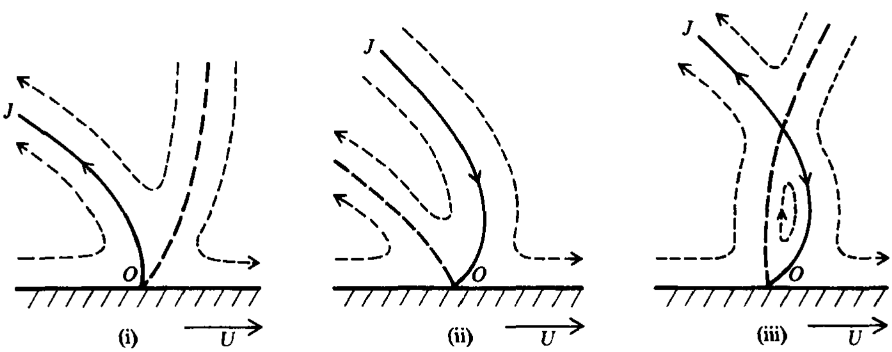

FIGURE 8. Sketches of streamlines for the situations where (i) $u_t > 0$ along the entire interface, (ii) $u_t < 0$ along the entire interface, and (iii) u_t changes sign along the interface. The liquid–liquid interface is the line OJ.

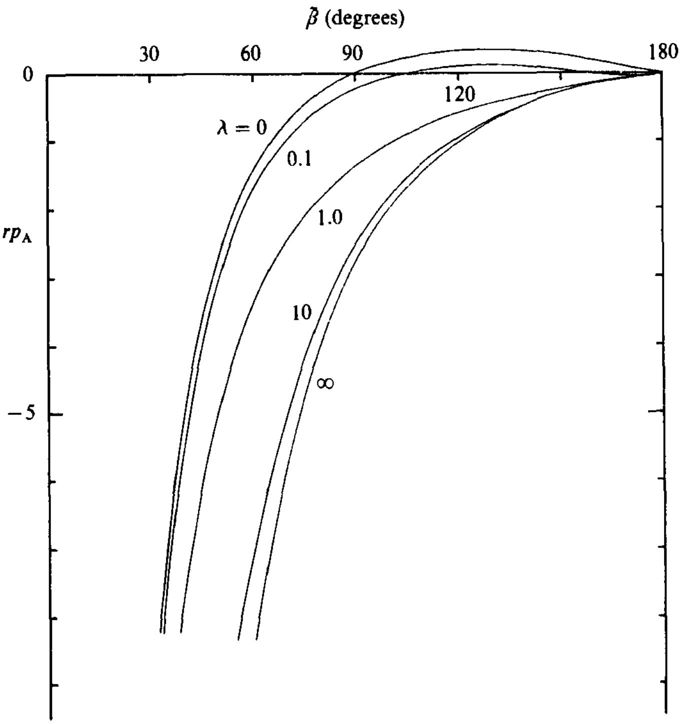

FIGURE 9. Value of rp_A on the solid surface (at $\phi = 0$) as a function of $\tilde{\beta}$ for various values of λ.

as a function of $\tilde{\beta}$ for various values of λ. It is noted that for $U > 0$, there is always a minimum value of p in the liquid A (i.e. behind the advancing contact line) at a value of ϕ which is plotted in figure 11. Also for λ greater than 6.73 ($(0.148)^{-1}$) and $U > 0$, there is for some range of $\tilde{\beta}$ a minimum value of p in liquid B, this occurring at the solid surface $\phi = \pi$.

From the values of the pressure on the solid surface given above and of the shear stress ($2r^{-1}E_A$ in liquid A, as $2\lambda r^{-1}E_B$ in liquid B, radially outwards) on the solid surface, the hydrodynamic force on the solid surface up to a distance R from the contact line is

$$2\boldsymbol{i}\int_s^R (E_A - \lambda E_B)\, r^{-1}\, dr - 2\boldsymbol{j}\int_s^R (C_A - \lambda C_B)\, r^{-1}\, dr, \tag{8.16}$$

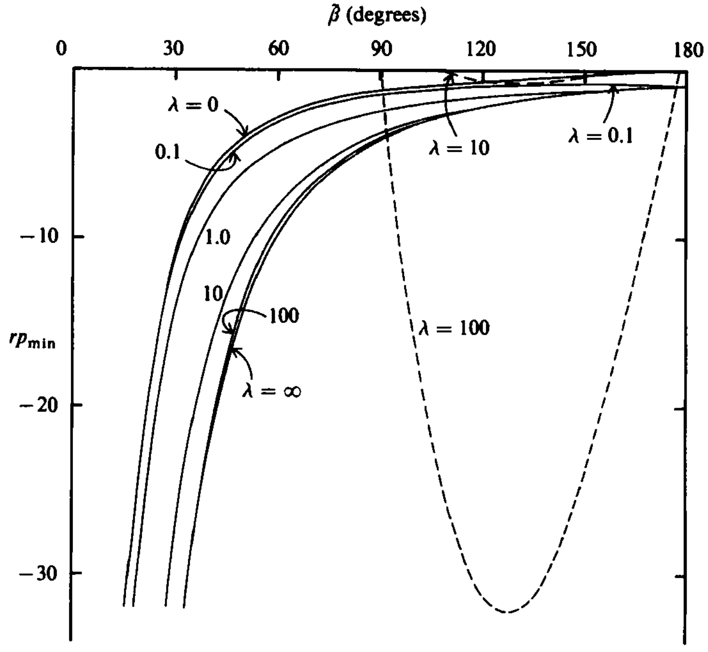

FIGURE 10. Value of $rp_{\min}$ as a function of $\tilde{\beta}$ for various values of λ (with $U > 0$) where $p_{\min}$ is the minimum dimensionless pressure. Only negative values have been plotted. The continuous lines represent the minimum values in liquid A, these occurring at the value of ϕ shown in figure 11. The broken lines represent the minimum values in liquid B, these occurring always at the solid surface $\phi = \pi$.

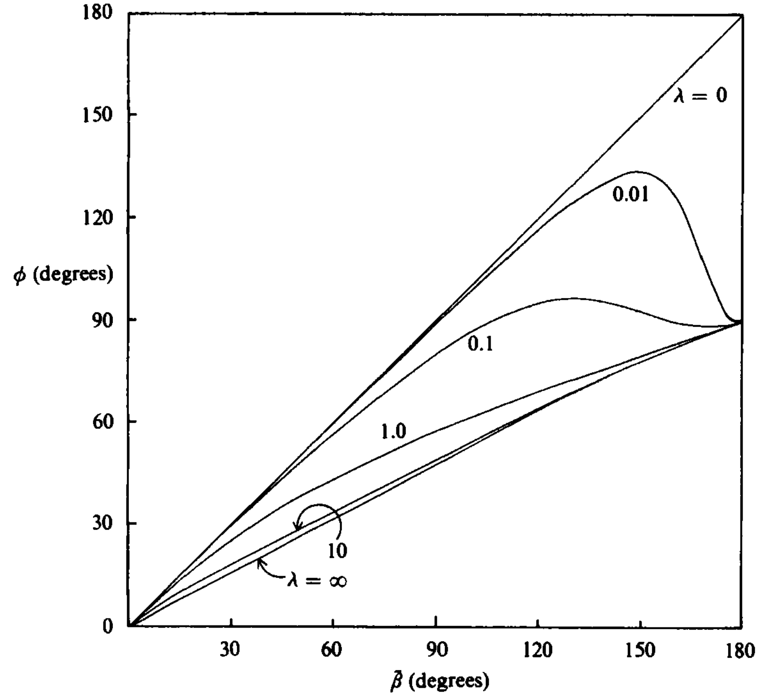

FIGURE 11. Values of ϕ at which the minimum pressure occurs in liquid A plotted as a function of $\tilde{\beta}$ for various values of λ (with $U > 0$).

where $\boldsymbol{i}$ and $\boldsymbol{j}$ are unit vectors parallel to and normal to the solid surface (in directions $\phi = 0$ and $\phi = \frac{1}{2}\pi$). This when combined with the interfacial tension force $Ca^{-1}(\cos\theta_w \boldsymbol{i} + \sin\theta_w \boldsymbol{j})$ on the solid surface gives the total force on the solid surface as

$$Ca^{-1}\left[\left\{\cos\theta_w - 2\int_{\theta_w}^{\theta_m} \frac{(\lambda E_B - E_A)}{f(\beta)}\,d\beta\right\}\boldsymbol{i} + \left\{\sin\theta_w + 2\int_{\theta_w}^{\theta_m} \frac{(\lambda C_B - C_A)}{f(\beta)}\,d\beta\right\}\boldsymbol{j}\right] + \dots \quad (8.17)$$

By either considering the momentum balance of the fluid within $r = R$ or by direct substitution of the values of C_A, C_B, E_A, E_B and $f(\beta)$ it may be shown that this force (8.17) is at order Ca^{-1} the same as the surface-tension force $Ca^{-1}(\cos\theta_m \boldsymbol{i} + \sin\theta_m \boldsymbol{j})$ exerted at $r = R$. However it should be noted that these forces are not identical at order Ca^0 because of the contribution of the hydrodynamic force at this order on the surface $r = R$.

The author wishes to thank one of the referees for his very helpful comments. This work was supported by the Natural Sciences and Engineering Research Council of Canada under grant A7007 and was undertaken in part at the Department of Mathematics, University College London, England and at the Department of Chemical Engineering, MIT, Cambridge, Mass., USA.

REFERENCES

Blake, T. D. & Haynes, J. M. 1969 *Colloid Interface Sci.* **30**, 421.

Burley, R. & Brady, P. R. 1973 *J. Colloid Interface Sci.* **42**, 131.

Burley, R. & Kennedy, B. S. 1976 *Chem. Engrg Sci.* **31**, 901.

Cherry, B. W. & Holmes, C. M. 1969 *J. Colloid Interface Sci.* **29**, 174.

Cox, R. G. 1983 *J. Fluid Mech.* **131**, 1.

Dussan, V., E. B. 1976 *J. Fluid Mech.* **77**, 665.

Dussan, V., E. B. 1977 *AIChEJ.* **23**, 131.

Dussan, V., E. B. 1979 *Ann. Rev. Fluid Mech.* **11**, 371.

Greenspan, H. P. 1978 *J. Fluid Mech.* **84**, 125.

Hocking, L. M. 1977 *J. Fluid Mech.* **79**, 209.

Hocking, L. M. & Rivers, A. D. 1982 *J. Fluid Mech.* **121**, 425.

Hoffman, R. L. 1975 *J. Colloid Interface Sci.* **50**, 228.

Huh, C. & Mason, S. G. 1977*a* *J. Colloid Interface Sci.* **60**, 11.

Huh, C. & Mason, S. G. 1977*b* *J. Colloid Interface Sci.* **81**, 401.

Inverarity, G. 1969 *Brit. Polymer J.* **1**, 245.

Jansons, K. M. 1985 *J. Fluid Mech.* **154**, 1.

Johnson, J. F. & Dettre, R. H. 1964 *Adv. Chem.* **43**, 112.

Kafka, F. Y. & Dussan, V., E. B. 1979 *J. Fluid Mech.* **95**, 539.

Kennedy, B. S. & Burley, R. 1977 *J. Colloid Interface Sci.* **62**, 48.

Lowndes, J. 1980 *J. Fluid Mech.* **101**, 631.

Ngan, C. G. & Dussan, V., E. B. 1982 *J. Fluid Mech.* **118**, 27.

Pisman, L. M. & Nir, A. 1982 *Phys. Fluids* **25**, 3.

Wenzel, R. N. 1936 *Ind. Engng Chem.* **28**, 988.